

THE ACQUISITION OF IMAGE DATA BY MEANS OF AN IPHONE MOUNTED TO  
A DRONE AND AN ASSESSMENT OF THE PHOTOGRAMMETRIC PRODUCTS

A University Thesis Presented to the Faculty  
of  
California State University, East Bay

In Partial Fulfillment  
of the Requirements for the Degree  
Master of Arts in Geography

By  
Jeffrey Curtis Miller

June 2016

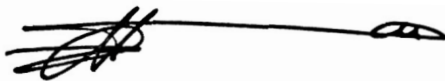
THE ACQUISITION OF IMAGE DATA BY MEANS OF AN IPHONE MOUNTED TO  
A DRONE AND AN ASSESSMENT OF THE PHOTOGRAMMETRIC PRODUCTS

By

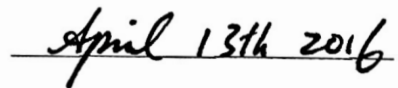
Jeffrey Curtis Miller

Approved:

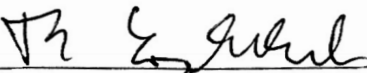
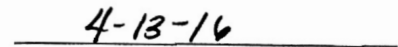
Date:



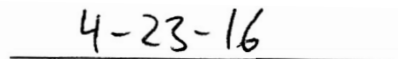
Dr. David Woo, Chair



Dr. Kerry Rohrmeir



Dr. Thomas Locherbach



## **Acknowledgements**

The author would like to acknowledge the following people and institution, without whom, this research and product would not have been possible. Dr. David Woo, thank you for your mentorship throughout the entire program and, especially, for agreeing to chair my thesis committee. Your support, advise, and encouragement were vital to my success. Your classes were informative and your teaching style always made the experience enjoyable. Dr. Thomas Loecherbach, thank you for agreeing to be on my committee and mentoring me throughout this process. You have been a great counselor throughout my career. I always appreciated how easy it was to talk to you. My career is further now than I could have imagined, and much of that success is due to the experience I gained under your guidance. Dr. Kerry Rohrmeier, I appreciate you accepting the role as one of my advisors. It is encouraging to see your passion for education and the student's success. Andras Ladai, thank you for your time, critique, and constant encouragement. You were an integral partner in coming up with solutions. Without your guidance, I would have struggled to produce results. Becky Morton and Alan Mikuni, thank you for your support and friendship. It took only a few months of knowing you to see how strong your passion was. In early 2014, you could have easily thought of me as another data analyst, but instead you believed in me. Since then we've formed a dynamic team, and I'm excited to grow our business together. Finally, thank you to California State University East Bay for providing an amazing program,

professors, resources, and academic setting that allowed me to research and create a thesis that contributes to an incredibly exciting new industry.



## **Table of Contents**

Acknowledgements	iii
List of Figures	vii
List of Tables	ix
Introduction	1
Part I. Photogrammetry	3
Chapter 1 – The History of Aerial Photography and Photogrammetry	3
Chapter 2 – Conventional Photogrammetry	9
Chapter 3 – UAS Photogrammetry	15
Part II. Data Collection Methodology	25
Chapter 4 – Hardware	25
Chapter 5 – Image Acquisition and Ground Control Collection	29
Part III. Data Processing Methodology	35
Chapter 6 – 3-D Model Construction	35
Part IV. Product Assessment	39
Chapter 7 – Model Tests/Accuracy Assessment	39
Chapter 8 – Image Quality	47
Chapter 9 – Mapping Solutions	49
Part V. Future Recommendations	53
Part VI. Conclusion	56



## **List of Figures**

Figure 1. Albrecht Meydenbauer's Survey Camera	3
Figure 2. Gasper Tournachon, First Aerial Photo	4
Figure 3. Fairchild's Mapping Camera and Manhattan Mosaic	5
Figure 4. Photogrammetry Timeline	7
Figure 5. Image Scale and Ground Sample Distance	11
Figure 6. Conventional Photogrammetry Aerial Cameras	11
Figure 7. Photo Overlap and Sidelap	13
Figure 8. Camera Focal Length Comparison	15
Figure 9. UAS Image Footprint	17
Figure 10. Conventional Photogrammetry Image Footprint	18
Figure 11. UAS Mapping Mission Flight Plan	19
Figure 12. Conventional Photogrammetry Mapping Mission Flight Plan	20
Figure 13. Structure from Motion	22
Figure 14. Conventional Vs UAS Photogrammetry Processing Workflows	24
Figure 15. UAS Hardware	25
Figure 16. iPhone 5S Mounted to Drone	27
Figure 17. Project Site - Lime Ridge Open Space	29
Figure 18. Project Flying Height and Image Scale	30
Figure 19. Project Flightlines	30

Figure 20. Control Point Targets	32
Figure 21. Control Points and Checkpoints Map	34
Figure 22. Project Image Processing Workflow, Step 1	35
Figure 23. Project Image Processing Workflow, Step 2 & 3	37
Figure 24. Map of Checkpoints Used for Accuracy Assessment	38
Figure 25. Image Overlap and Coverage	40
Figure 26. Vertical Offsets Mapped	44
Figure 27. Vertical Residuals Vs Absolute Heights	45
Figure 28. M03 TIN Vs Checkpoints TIN	46
Figure 29. M03 Vs Checkpoints Change Map	46
Figure 30. Jello Effect on Image Quality	47
Figure 31. Derived Mapping Solution – Orthophoto Mosaic	49
Figure 32. Derived Mapping Solution – Point Cloud of Bare Earth	50
Figure 33. Derived Mapping Solution – Digital Terrain Model	51
Figure 34. Derived Mapping Solution – Contours	52

## **List of Tables**

Table 1. UAS Vs Conventional Photogrammetry Flight Plan Comparison	21
Table 2. iPhone 5S Camera Specifications	26
Table 3. Project Flight Statistics	31
Table 4. Digital Terrain Model Characteristics Breakdown	39
Table 5. Horizontal Positional Accuracy	41
Table 6. Vertical Positional Accuracy	42

## **Introduction**

At the “UAS Mapping Reno 2014” conference, disruptive technology was a term used to describe the effect drones are having on people’s everyday lives. Depending on the situation, this description reigns true. A drone could be hovering over your backyard, spying through your living room window, or scaring your dog from above. All of these scenarios would be a disruption to you, your dog, your neighbors, and community. A Kentucky man took matters into his own hands when he shot down a disruptive drone (Man Shoots Down Drone Hovering over House 2015).<sup>1</sup> This paper, however, is about how drone technology is disrupting, transforming, and revolutionizing an entire industry. That industry is mapping, and more specifically, the mapping methodology this paper focuses on is photogrammetry.

Photogrammetrists have been using aerial photographs to create maps since the beginning of the twentieth century. Drones, or unmanned aircraft systems (UAS) are changing the way aerial photos are taken. The emergence of autonomously capable UAS equipped with consumer-grade cameras is redefining how aerial data is collected (Anderson, 2013).<sup>2</sup> By combining traditional photogrammetric techniques and UAS technology, the mapping industry is embarking on an aerial photogrammetry revolution. If the accuracy and quality of UAS aerial photography is proven to meet the standards of the mapping industry, UAS will empower photogrammetric professionals, and non-professionals, to view and map the world significantly cheaper and faster. This paper

explores whether or not a consumer-grade UAS can produce mapping products that meet those standards.

## Part I. Photogrammetry

### Chapter 1 – The History of Aerial Photography and Photogrammetry

The first person to use photographs for surveying applications was German building surveyor Albrecht Meydenbauer. His initial discovery occurred by accident in 1858 while performing an architectural survey on a cathedral. Working on the facade of the cathedral, Meydenbauer had a traumatic experience when he almost fell to his death. He then realized his direct measurements could be replaced by indirect measurements of photographs of the cathedral (A Look Back 2007).<sup>3</sup>

His findings would lead Meydenbauer to devote all of his time to developing photogrammetric methods. He designed cameras with technical solutions that formed the basic elements of all photogrammetric cameras in the future. Figure 1 shows one of Meydenbauer's first cameras. A few of Meydenbauer's developments included:

- an image plane with a mechanical frame

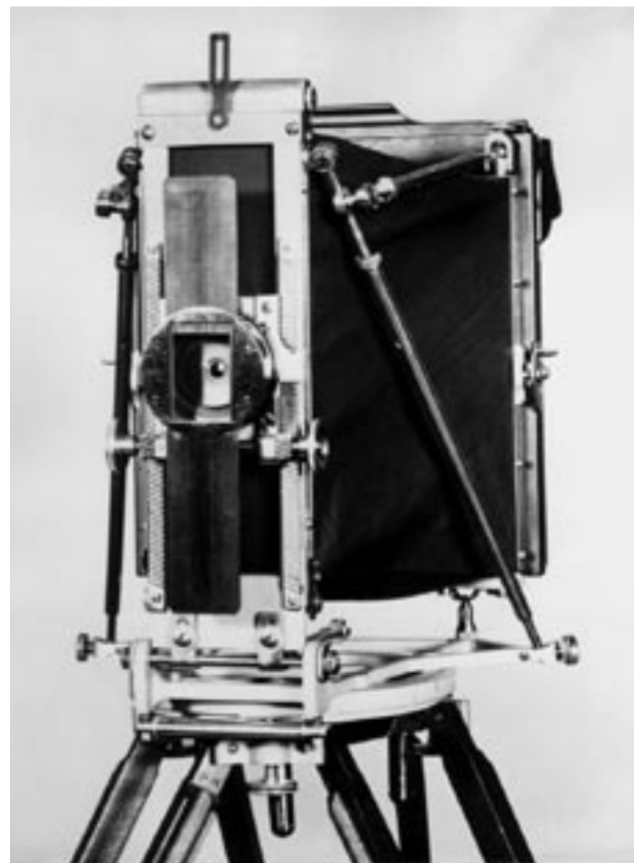


Figure 1  
Albrecht Meydenbauer's Survey Camera  
Source: A Look Back



- integration of an image coordinate system
- a compact camera with a calibrated or fixed focal length
- camera adjustments to the horizontal and vertical coordinate axis.

The term photogrammetry was born in the summer of 1867 when Meydenbauer successfully performed architectural and topographical surveys using photography.

Nevertheless, it took 25 years for Meydenbauer's photogrammetry to be accepted as a legitimate survey method by the German parliament due to concerns over accuracy.

Established on April 1, 1885, The Royal Prussian Photogrammetric Institute was the first photogrammetric institution in the world (A Look Back 2007).<sup>3</sup>

The first aerial photograph (Figure 2) was taken from a balloon over Paris in 1858 (Lillesand et al., 2008, 63).<sup>4</sup> French photographer Gaspar Felix Tournachon experimented for 3 years before being able to produce aerial photographs. His original idea (patented "Nadar") was to use the aerial photography for mapping and surveying. As technology improved, other photographers took to the skies. Some of the earliest camera-carrying platforms included kites, rockets, and even pigeons. The first aerial photographs from an airplane were taken over Italy by Wilbur Wright in 1909. A few years later, aerial photography by plane became extremely useful for



Figure 2  
Gaspar Tournachon, First  
Aerial Photo  
Source: Professional Aerial  
Photographers Association

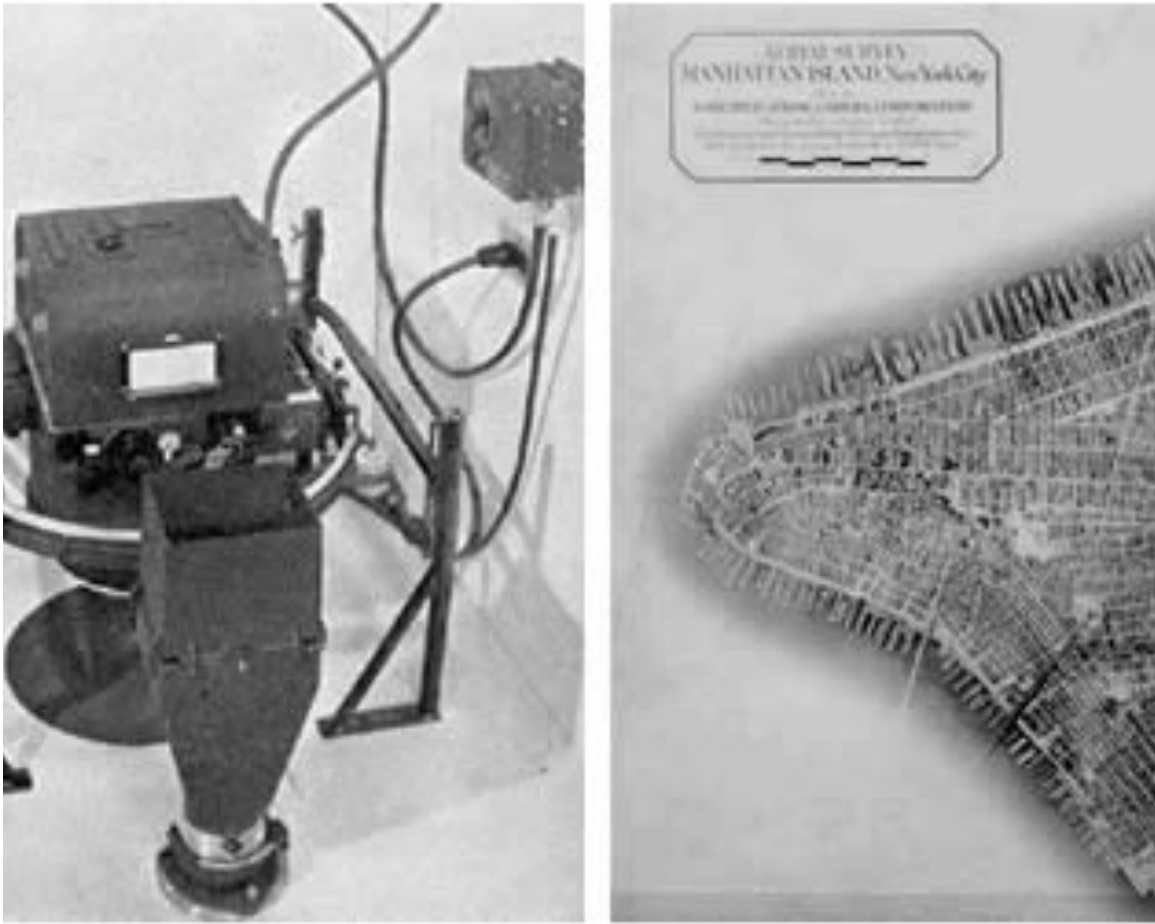


Figure 3  
Fairchild's Mapping Camera and Manhattan Mosaic  
Source: Professional Aerial Photographers Association

military applications during World War I. Cameras designed specifically for aerial mapping were being produced to make battle-front maps (History of Aerial Photography 2015).<sup>5</sup>

Following the end of the war, many former military photographers turned aerial photography into a legitimate commercial business by developing their own aerial survey and mapping firms (Lillesand et al., 2008, 64).<sup>4</sup> Like Tournachon, Sherman Fairchild saw mapping as a befitting application, and designed specialty cameras for airplanes. The first

small-scale (large area) photo-mosaic was taken by Fairchild over Manhattan Island. By stitching 100 overlapping photos together (Figure 3), Fairchild produced a map that was widely popular with New York City agencies and businesses. In comparison to traditional land surveys, aerial methods proved less expensive. Since then, aerial photography has been an important utility for mapping and surveying professionals (History of Aerial Photography 2015).<sup>5</sup>

The term “photo-gram-metry” is derived from three Greek words: photos—meaning light, gramma—meaning something drawn, and metron—meaning to measure (McGlone et al., 2004, 1).<sup>6</sup> Many advancements in photogrammetry occurred during the period between WWI and WWII. Most of the progress occurred in Western Europe, and by the end of the 1930’s, photogrammetry was being practiced around the world as an advanced technology.

Photogrammetry became widely used in the United States following the founding of the American Society of Photogrammetry and Remote Sensing (ASPRS) in 1934. To this day, ASPRS is the outlet for the advancement of geospatial technologies by publishing map standards, journals, books, and professional and academic workshops. They are responsible for vetting photogrammetry professionals through classes and certification programs (ASPRS Mission Statement 2015).<sup>7</sup> Following the Second World War, photogrammetric development shifted to the expanding scientific and industrial United States. Mathematical modeling became the basis for the analytical expression of geometric relationships of objects in photographs. Developments in aerotriangulation

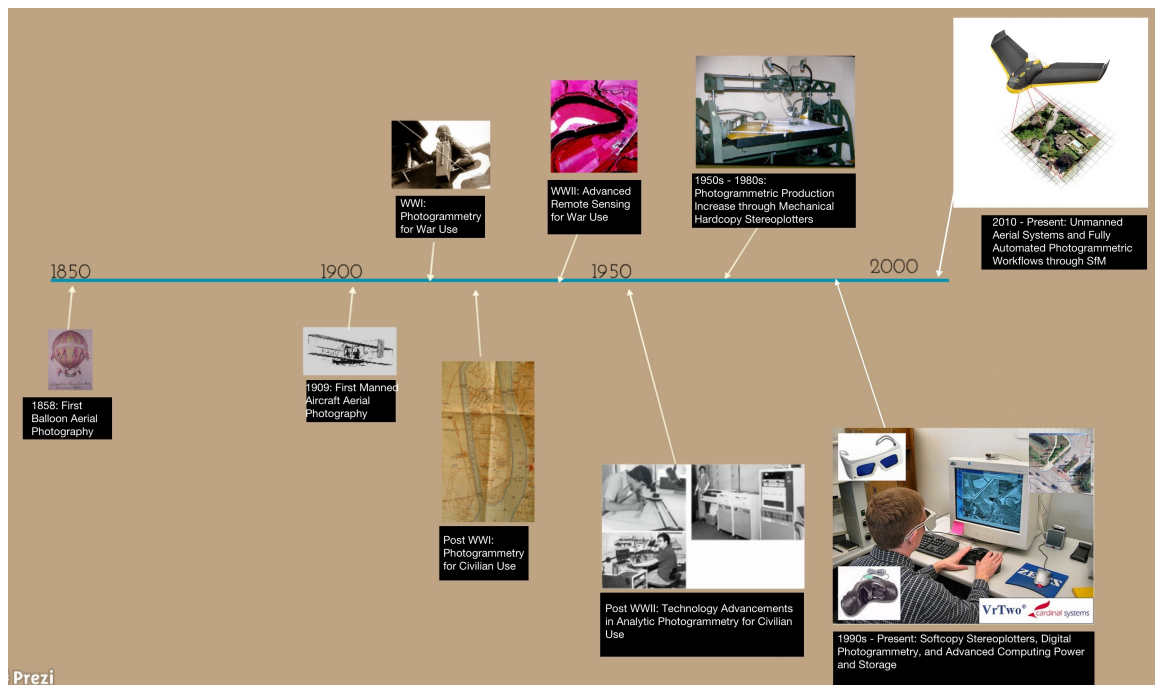


Figure 4  
Photogrammetry Timeline  
Source: Guarneri, J. (2012)<sup>8</sup>

(AT) methods based on the concept of space resection, determining a least squares solution for the location of unknown photocoordinates, automated the process of map production. The advancement of computers capable of churning thousands of mathematical algorithms and enhancements to mapping cameras further improved efficiency (McGlone et al., 2004, 9).<sup>6</sup>

Like with many facets of society, advancements in computing power and storage had a substantial impact on photogrammetry in the latter part of the 20th century. Data could be written and recorded in a digital format increasing speed and expanding storage. It was not until the advancement of digital cameras, however, that a

photogrammetric process could become entirely digital. Analytical AT improved as well consequently shifting the photogrammetric workflow to become fully automated.

Decades later, the digital age created a radical shift in how data was stored and processed. This meant the elimination of film and hardcopy prints. Recent technology developments are creating rifts, shifts, and new concepts. These technologies are Structure from Motion and Drones. Figure 4 breaks down the evolutionary timeline of photogrammetry.

## Chapter 2 – Conventional Photogrammetry

Lillesand et al. (2008)<sup>4</sup> defines photogrammetry as "the science and technology of obtaining spatial measurements and other geometrically reliable derived products from photographs" (123). There are numerous methods of deriving products using photogrammetry. Aerial photogrammetry is the method of flying over an area with a camera pointed at nadir or straight down (Lillesand et al., 2008, 123).<sup>4</sup> This is the most common method for producing mapping solutions and terrain observations. Geometrically correct models can also be produced by angling a camera at an oblique angle(s). This can be done aerially or terrestrially, as long as sufficient photo overlap exists. Virtually anything, like a standing structure or building, or the geomorphology of a watershed, can be modeled using photogrammetric methods. For the remainder, this author will refer to aerial photogrammetry simply as photogrammetry since the entire focus will stem from an aerial perspective.

Before comparing conventional photogrammetry (CP) to UAS photogrammetry, it is important to consider the factors that impact both methods similarly. Lillesand et al. (2008)<sup>4</sup> describes those factors as the following:

- Image Scale - Based on flying height above ground and terrain elevation, the image scale can be used to make ground measurements relative to corresponding photo measurements.
- Object Displacement - Unlike maps, aerial photographs do not show a true plan or top view of objects unless taken directly above the object. Object displacement causes

objects, especially taller ones, to lean from their bases. Height measurements can be made, however, by factoring in the scale and amount of lean an object has. This practice is especially accurate when measuring an object or ground elevation in two overlapping images.

- Ground Control Points (GCP) - GCPs are actual measurements made on the ground by a land survey crew. They are paramount to the positional accuracy and ground truth of any photogrammetry project.
- Flight Plan: Proper flight planning must take place to ensure the desired products can be produced in any photogrammetry project. Information about the camera, image scale, and photo overlap are all important factors in proper flight planning (119-121).

Image scale is explained in Figure 5. The ground sample distance (GSD) or pixel resolution and the specifications of the camera are the determining factor of how high above the ground (H) the plane will fly and how large the image footprint (g) will be (Falkner et al., 2002, 29).<sup>9</sup> GSD is the image pixel size expressed in units of the ground. For example, a 1" GSD would mean that every pixel in the processed imagery would represent an inch on the ground. Flying height can be determined by the following formula:

$$H = \text{GSD} \times f \div \text{pixel size}$$

$$\text{CP Example: } H = 1'' \times 6'' \div 0.0006'', H = 10,000'' \text{ or } 833'$$

As displayed in Figure 6, aerial photography for CP is acquired using a large format camera (either film or digital) that is calibrated for mapping and usually mounted

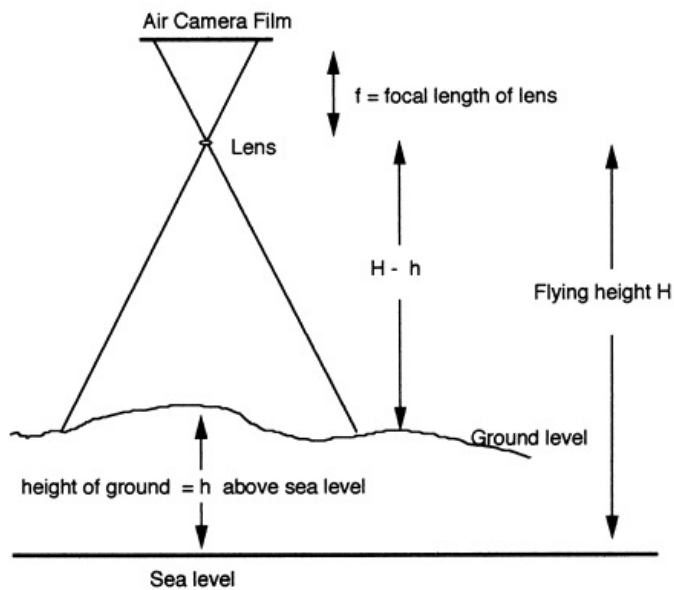


Figure 5  
Image Scale and Ground Sample Distance  
Source: FAO



Figure 6  
Conventional Photogrammetry Aerial  
Cameras (Top to Bottom) – RC30 Film  
Camera, UltraCamD Digital Camera  
Source: New Tech Services Inc.

in a Cessna aircraft. These cameras can cost as much as \$1,000,000. Flight services can be expensive as well due to fuel costs, pilot time, and travel time.

Conventional flights are also dependent on good weather. Many CP projects still fly using an RC30 mapping camera with a 6" focal length and 15  $\mu$  or 0.0006" pixel size. As seen in the above example, a 1" desired GSD would require the plane to fly 833' above ground level (AGL). This is a limitation of CP because in most areas of the U.S., the minimum flying height of a commercial aircraft is 1,000' (Minimum Safe Altitudes, 2002).<sup>10</sup> Therefore, the highest resolution CP imagery acquired is usually 2"-3".



An advantage of the CP acquisition is the large image footprint. The following formula explains how to determine g:

$$g = (\text{image pixels in row} \times \text{GSD}) \times (\text{image pixels in column} \times \text{GSD})$$

CP Example:  $g = (15,000 \times 1'') \times (15,000 \times 1'')$ ,  $1,250' \times 1,250'$ ,  $g = 1,562,500'^2$ ,  $g = 36$   
acres

With a 1" GSD (which we've already determined is most likely not doable), a CP image footprint will cover roughly 36 acres. That's enough coverage to map a strip mall, track home development, or other site mitigation. Large image footprints make CP ideal for large areas of interest (AOI) (Falkner et al., 2002, 30).<sup>9</sup>

Image overlap plays a significant role in photogrammetry. To guarantee proper coverage, photographs must overlap in two directions, in the line of the flight and between adjacent flights. Aircrafts flight paths are predetermined to ensure successive overlap of camera exposures. Figure 7 illustrates a conventional photogrammetric project requiring a 60% overlap and 30% sidelap between each exposure and flightline (Lillesand et al., 2008, 128).<sup>4</sup> The air base is the distance between photo centers and determines the amount of forward overlap between exposures. In CP, the overlapping area creates a stereomodel and gives the three-dimensional effect necessary for mapping.

Ground control points are necessary for providing an accurate ground truth to aerial photos. The conventional method is to have a licensed Professional Land Surveyor (PLS) gather both horizontal and vertical ground measurements (Ogaja, 2011, 49).<sup>11</sup> For use with photogrammetry, photo identifiable targets are laid down or spray painted on a

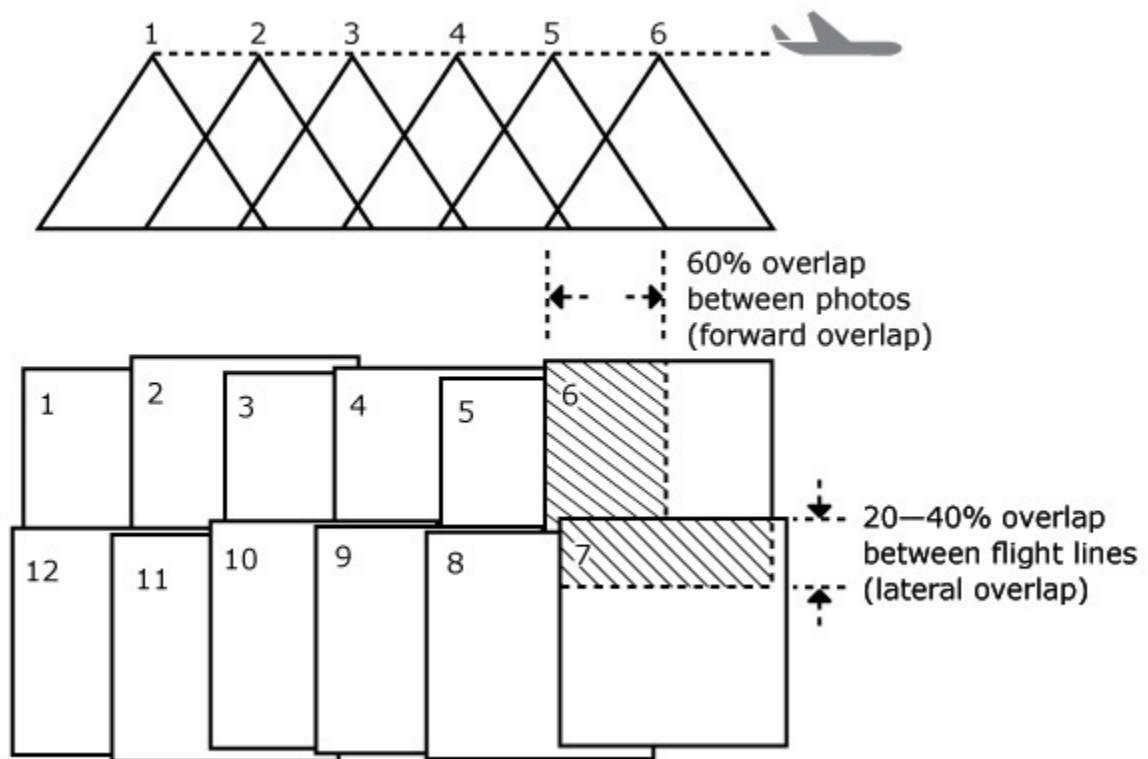


Figure 7  
Photo Overlap and Sidelap  
Source: UAS Mapping and 3D Modeling

surface and the PLS measures the ground in the center. Aerotriangulation is the method of orienting images to the proper geographic location (i.e., determining their position and rotation, in space) (Lillesand et al., 2008, 189).<sup>4</sup> In CP jobs that only require one or two exposures, the GCPs are sufficient enough for image orientation. Jobs that require hundreds or thousands of images, however, would also require hundreds or thousands of GCPs, which would not be cost-effective. AT bridges areas without ground control and reduces the number of ground control points needed. A pair of overlapping images can be relatively oriented to one another by measuring the exact same ground object (called a tie

point) in each of the corresponding images. Modern systems can efficiently create tie points for the entire block of images through automatic point measurement. The GCPs complete the orientation of the block through methods of space resection. The flight GPS and inertial measurement unit (IMU) data aid in the creation of the bundle-adjustment (Lillesand et al., 2008, 180).<sup>4</sup>

### Chapter 3 – UAS Photogrammetry

While conventional photogrammetry has been practiced for over 100 years, photogrammetry from an unmanned system or drone is relatively new. Technology advancements in drone hardware (primarily the integration of onboard GPS), camera miniaturization and sensor quality improvements, and a number of innovative software packages have created the perfect storm to disrupt the mapping industry, and in particular photogrammetry. While many of the foundational principles still apply, a number of stark differences are present between CP methods and UAS.

Image scale and GSD vary not only from CP, but from one UAS project to the next. Pixel resolution in CP has been generally uniform over the last few decades due to minimum flying height limitations of a manned aircraft. Drones are not hindered by this. It is, in fact, the opposite limitation facing UAS pilots. Rather than limit how fine a GSD can be, drones are currently restricted to fly below 400 ft AGL making it the GSD coarseness that is (Colomina et al., 2014, 81).<sup>12</sup> Instead of acquiring GSD in inches and feet, UAS photogrammetry is often acquired in centimeters. Consider the scale of a small drone and off-the-shelf (OTS) camera compared to a Cessna and an RC30. Figure 8 demonstrates the difference in camera focal

OTS  
Focal length  
5 mm

RC30  
Focal Length  
152 mm

Figure 8  
Camera Focal Length Comparison

lengths between an RC30 CP camera and an OTS Canon. The CP camera has a focal length of 6" or 152 mm where the Canon only has a focal length of 5 mm (Lieca RC30 Aerial Camera System, 2016). Pixel size is also drastically smaller. The RC30's has a pixel size of 15  $\mu$  compared to 1-2  $\mu$  for OTS cameras (Crisp, 2013).<sup>14</sup> Figuring out the flying height for a UAS photogrammetry project with a GSD of 1" can be done using the same formula in chapter 2:

$$\text{UAS Example: } H = 1'' \times 0.197'' (5 \text{ mm}) \div 0.000059'' (1.5 \mu), H = 3,339'', H = 278'$$

Since drones can fly low, they can fly under low clouds. Contrary to CP, however, Colomina et al. determined it's best to acquire UAS data during an overcast day (82).<sup>12</sup> UAS imagery is more subject to differences in image quality exposure caused by changing sun reflectance. A grey homogeneous sky ensures light is reflected uniformly throughout the UAS image dataset. Hazardous weather and wind are more problematic for UAS because of their light weight. Wind can also cause quality issues to imagery (Colomina et al., 2014, 81).<sup>12</sup>

Similar to flying height, image footprint is drastically smaller for UAS photogrammetry. Not only do OTS cameras have smaller pixel sizes, they have less pixels per row and column (Crisp, 2013).<sup>14</sup> An RC30 has 15,000 pixels per row and per column. Off-the-shelf cameras generally have around 4,000 pixels per row and per column. The following formula from chapter 2 can be applied to an OTS camera with a 1" GSD:

$$\text{UAS Example: } g = (4,000 \times 1'') \times (4,000 \times 1''), 333' \times 333', g = 111,089'^2, g = 2.5 \text{ acres}$$

The comparisons between g for CP and UAS photogrammetry are visualized over the CSU East Bay campus in figures 9-10. Figure 9 is an example of a footprint from a Canon with a 5 mm focal length and 1.5  $\mu$  pixel size (the purple box represents the footprint). This example is over the CSU East Bay campus library. As shown, one image from the Canon does not cover the entire building. The footprint for the Canon is 2.5 acres.



Figure 9  
UAS image footprint (Purple Box) from example Canon OTS camera



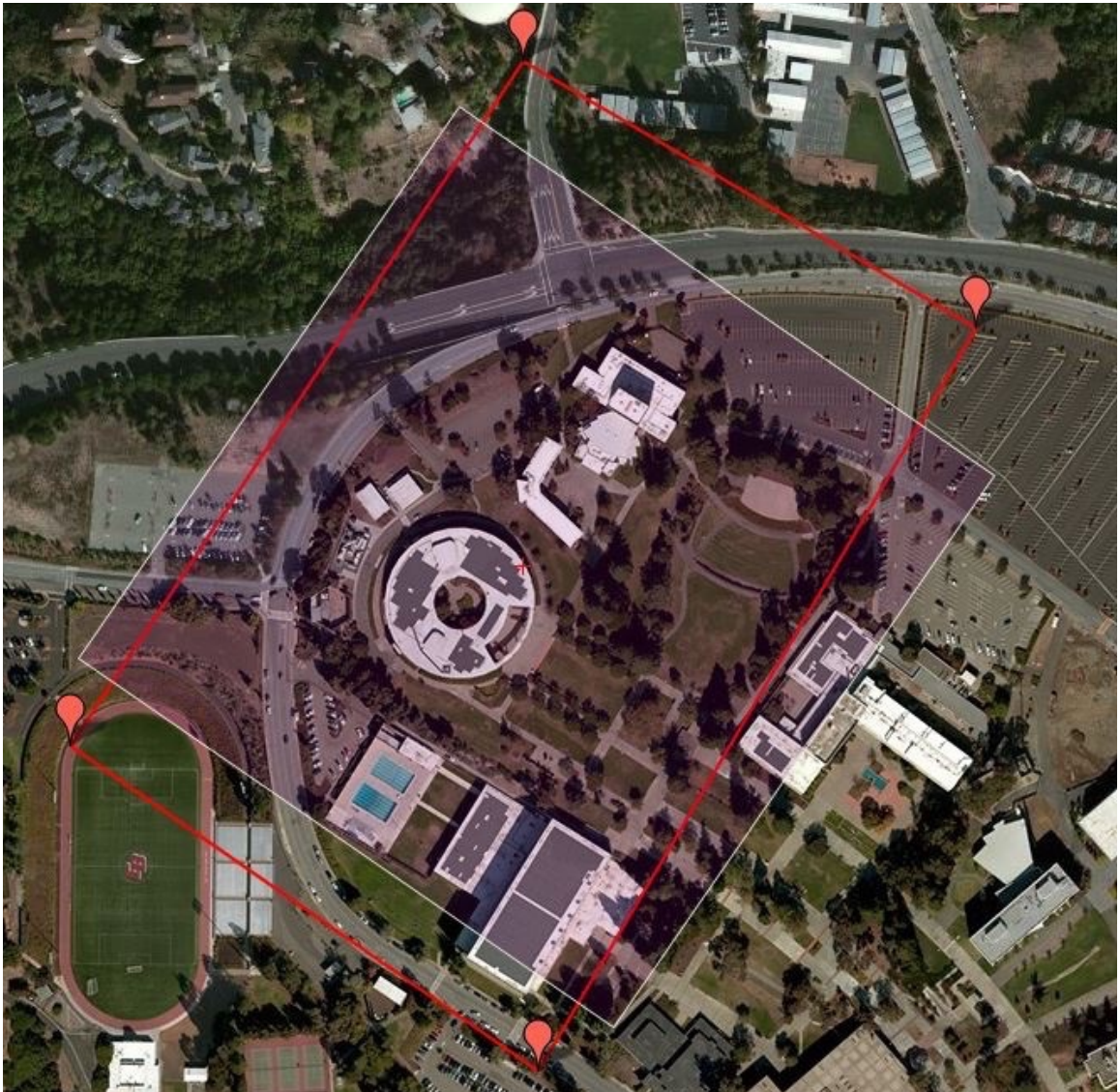


Figure 10  
Conventional Photogrammetry image footprint (Purple Box) from exampleRC30





Figure 11

UAS Mapping Mission Flight Plan

Red Polygon Represents Area of Interest, Yellow Lines Represent Flightlines

Example: 11 Flightlines, 239 Photos (179 acres, CSUEB Campus)





Figure 12  
Conventional Photogrammetry Mapping Mission Flight Plan  
Red Polygon Represents Area of Interest, Yellow Lines Represent Flightlines  
Example: 3 Flightlines, 18 Photos (179 acres, CSUEB Campus)

Figure 10 illustrates the contrary footprint of an RC30 CP camera. The RC30 camera has a g of 36 acres, enough to cover about 25% of the campus. Figures 11-12 compare the amount of photos needed to map roughly 179 acres of the entire CSUEB campus using a

conventional 60% overlap and 30% sideslip metric. In both figures, the yellow lines represent the flightlines and the red polygon represents the area of interest. In Figure 11, The UAS would need to fly 11 flightlines and capture 239 photos. In Figure 12, the RC30 would need 3 flightlines and capture 18 photos. That's equal to 1,300% more images needed for the UAS! A comprehensive review of this statistical comparison can be found in Table 1.

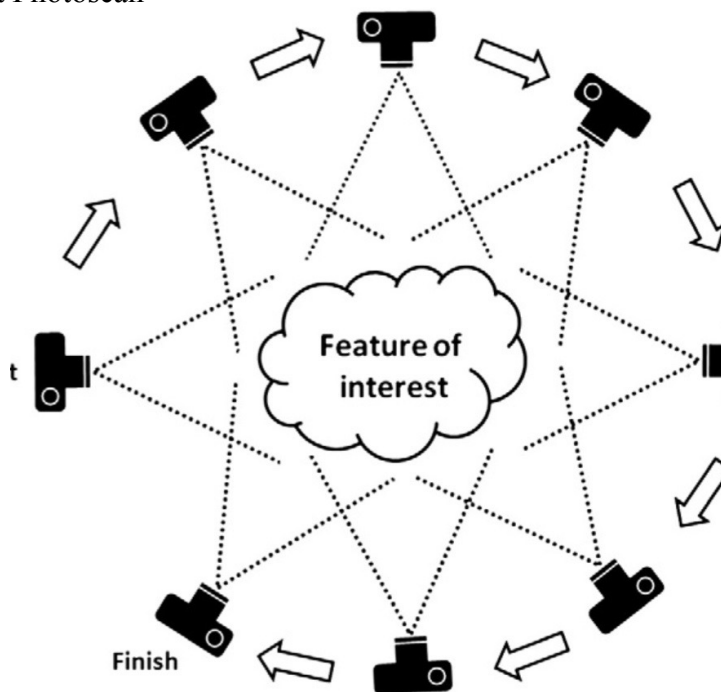
Table 1	Canon Off-the-Shelf Camera	RC30 Mapping Camera
System	Drone	Cessna
Focal Length (f)	5 mm	152 mm
Image Pixel Size	1.5 $\mu$	15 $\mu$
Pixels per Row/Column	4,000 x 4,000 (average)	15,000
Flying Height AGL for 1" GSD (H)	278 ft	833 ft
Image Footprint for 1" GSD (g)	2.5 acres	36 acres
Photos needed to cover 179 acre CSUEB campus (60% overlap 30% sidelap)	239	18

Table 1  
UAS vs. Conventional Photogrammetry Flight Plan Comparison

Unmanned systems image data is processed differently than conventional photogrammetry. Key elements such as overlap/sidelap, sun angle, and GCPs remain fundamentally important to UAS photogrammetry. But the aerotriangulation, 3-D model

creation, and image mosaic workflows are more automated. The processing workflows of conventional photogrammetry and UAS are explained in detail in Figure 14 below. The emergence of Structure from Motion (SfM) has made this possible. Westoby (2012)<sup>15</sup> defines SfM as a photogrammetric technique that shares fundamental elements of CP like overlap and GCPs, but differs in that scene geometry and camera orientations are solved simultaneously using high redundancy image matching. Instead of determining 3-D camera positions through space resection, the high redundancy allows for automatic identification of matching features in multiple images. Object coordinates are then estimated iteratively using non-linear least-squares minimization (Westoby et al., 2012).<sup>15</sup> Scene modeling is conducted in the reverse method of CP, and the automation saves time

Figure 13  
Structure from Motion  
Source: Agisoft Photoscan



in comparison to manually extracted data from a compiler using a stereo plotter. Structure from Motion's popularity did not start with aerial mapping. Microsoft's cloud processing engine Photosynth, a service for users interested in creating 3-D models from everyday photos, started the SfM movement (Snavely et al., 2008).<sup>16</sup> Over the last few years, the rise in popularity of drones with OTS cameras and SfM technology formed the perfect marriage for an innovative platform for photogrammetry and aerial mapping.

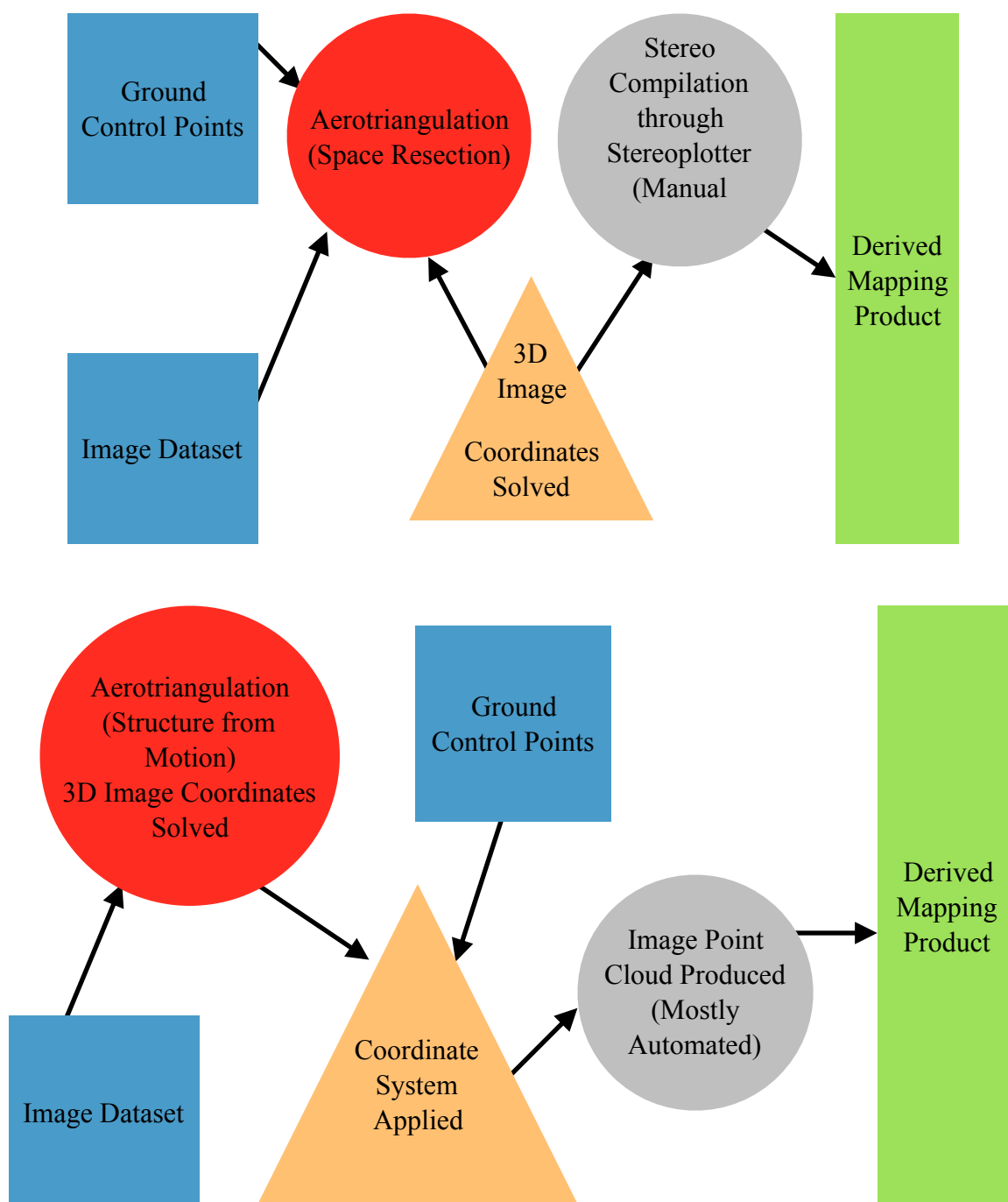
As illustrated in Figure 13, SfM relies on highly redundant data, thus a higher amount of photo overlap/sidelap is suggested by SfM software vendors (Agisoft Photoscan Users Manual, 2013).<sup>17</sup> The perfect percentage is debatable since research on this topic is still very new. This author will explore this topic in greater detail in the methodology section.

Figure 14

Conventional vs. UAS Photogrammetry Processing Workflows

Top Represents CP, Bottom Represents UAS

Colors Explained (Both Examples): **Blue** - Inputs, **Red** - Aerotriangulation, **Tan** - Ground Truth, **Grey** - Method of Producing Data, **Green** - End Solution



## Part II. Data Collection Methodology

### Chapter 4 – Hardware

The two factors that were most important when choosing a drone were price and autonomous flight capability. The IRIS quadcopter, made by 3D Robotics (3DR), was a ready-to-fly (RTF) package meaning the remote controller, battery, charger, etc. were included and programed. At the time of purchase, the retail price was \$749.

The quadcopter platform is the most popular modern drone in the world. They are incredibly stable and easy to learn compared to helicopter or fixed-wing counterparts. In order to fly in an accurate lawnmower style flight path, it was important that the IRIS have the option for easy autonomous flight. Built in components such as GPS, an inertial measurement unit (IMU), and a compass provide the hardware for autonomous flight (IRIS+, 2016).<sup>18</sup>

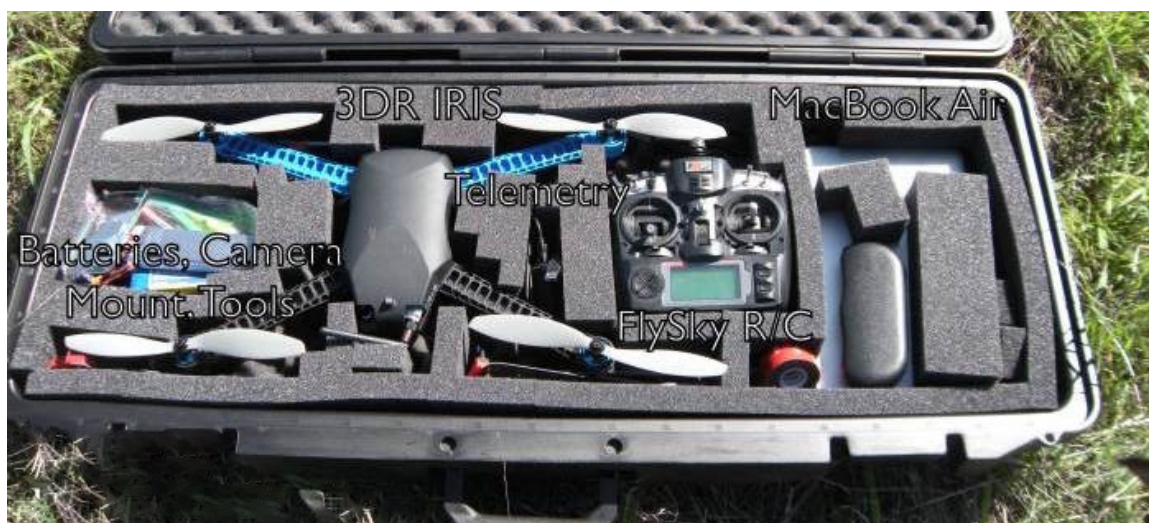


Figure 15  
UAS Hardware  
Left to Right: Accessories, 3DR IRIS Drone, RC Controller, Laptop (Ground Station)



Mirroring hardware with software is the final step in completing the unmanned “system.” The software used for flight planning and ground station is called Mission Planner. Mission Planner is an open source software package designed to work with 3DR products. The supplied telemetry antenna enables any laptop to become a flight planner and ground station. A photogrammetry extension is built into Mission Planner and provides statistical information about the mission. A heads-up display provides real-time flight data in the field. Integrating the ground station completes the transformation of an unmanned vehicle to an unmanned aircraft system. Figure 15 illustrates the system including the IRIS drone, an RC controller, and a laptop.

At the time of this writing, there are numerous vendors selling RFT UAS with built on cameras. This was not so much the case in 2013. While most research was being conducted using a GoPro camera, it was avoided because of its low quality image sensor and wide angle lens. The iPhone revolutionized cell phones and each new model is more

Sensor Type	CMOS rolling shutter
Focal Length (f)	4.1 mm
Image Sensor Size	3.4 mm
Image Pixel Size	1.4 $\mu$
Pixels per Row/Column	3,264 x 2,448

Table 2  
iPhone 5S Camera Specifications



Figure 16

#### iPhone 5S Mounted to Drone

Note: The camera is mounted to the bottom of the drone. The camera is therefore pointed nadir or downward to the ground. The top of the drone is facing the table.

popular than the previous. Camera upgrades are common for each new model. An iPhone 5S was used for this project. The sleek design and 4 oz weight matched well with the IRIS. Table 2 displays important specifications about the 5S camera (Crisp, 2013).<sup>14</sup>

There were no commercial mounts available for an iPhone or drone of any kind. By mixing and matching parts from various vendors, the author was able to develop an adequate camera mount. To hold the camera in place, the iPhone was fit backwards in a thin and clear phone case. This ensured the camera was always pointed toward or within



a few degrees of nadir (pointed straight down towards the ground) while in flight. The camera mounted to the drone is shown in Figure 16. The case was then screwed to a fixed anti-vibration mount. The importance of the anti-vibration mount is in Chapter 8.

## Chapter 5 – Image Acquisition and Ground Control Collection

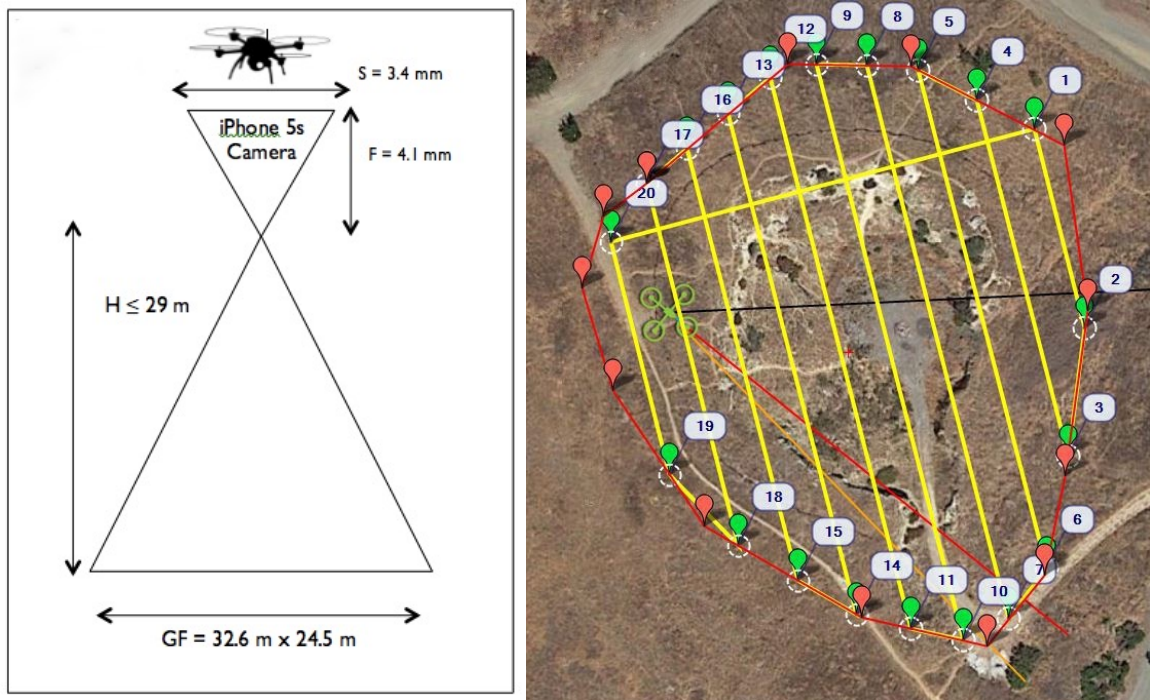
The area chosen for this project was important in that it had to have varying topography and vegetation. But it still had to be easily accessible, away from an urban area, and the proper size for one flight of the UAS. Lime Ridge Open Space in Concord, CA is a former quarry site that was decommissioned in 1946 and converted to an open space in 1974. It is the second largest open space in California. In the late 19th and early 20th centuries, limestone was mined in this area leaving behind numerous ruins (Lime Ridge Open Space 2012).<sup>19</sup> The quarry off Treat Blvd. fit all of the project needs. The AOI is roughly 2.5 acres. Figure 17 displays various photographs taken at the project site. There is a 30 meter difference from the base to the crest as illustrated by the photos.



Figure 17

Project Site - Lime Ridge Open Space

Note: Various photos taken at the base and crest of the project site.



Figures 18 & 19 (Left to Right)

Project Flying Height and Image Scale, Project Flightlines

Note: To achieve 1 cm GSD the drone was flown no higher than 29 m. Ten flightlines were needed to achieve the recommended 80% overlap and 40% sideslap.

Image data was collected on March 7th, 2014. The flight took place in the afternoon between 1:40-1:50pm PST. Wind speed was less than 5 mph and the day was sunny with no cloud cover. Previous examples and comparisons centered around acquiring image data with a 1" GSD. Pixel resolution can be finer than that, however, with a UAS. Higher resolution GSD requires more flightlines and images due to the size of the image footprint. The selected GSD for the project was 1 cm. Additionally, the data was to be processed using SfM software, so the overlap and sideslap were 80% and 40% (Agisoft Photoscan Users Manual, 2013).<sup>17</sup> For a 1 cm GSD, the UAS was flown at  $\leq 29$  m (95 ft) AGL. Figure 18 displays the flying height ratio, and Figure 19 illustrates the

GSD	1 cm
Flying Height (H)	$\leq 29$ m
Image Footprint	798 m <sup>2</sup> or 0.20 acres
Overlap	80%
Sidelap	40%
Number of Flightlines	10
Distance Between Flightlines	9.8 m
Air Base	7.35 m
Photos per Second	1
Total Number of Photos	236

Table 3  
Project Flight Statistics

flightlines for the project. Once the flight plan was designed and programmed into the IRIS' autopilot, the camera shutter was activated using an onboard app called CameraSharp (CameraSharp, 2015).<sup>20</sup> The CameraSharp app was designed to take time-lapse photography and has an option for setting the camera shutter to snap a photo at set intervals. The drone speed was set to 7 m/s which meant the camera needed to take a picture every second in order to achieve 80% or better overlap. CameraSharp does enable the user to modify camera settings such as auto-white balance, auto-focus, etc. (CameraSharp, 2015).<sup>20</sup> Through previous testing, the author found leaving these settings as default produced the best and most consistent photos. Activating the camera shutter through the app was done on the ground before take-off, and deactivating it occurred after

landing. Photos taken that were not part of the autonomous portion of the flight were not used during processing. A breakdown of the project flight statistics is in Table 3.

The author used to work for a professional geomatics company and had friends with experience and equipment for land surveying. During the morning before the flight, a Professional Land Surveyor (PLS) using Real Time Kinematic (RTK) GPS equipment

surveyed the project site. RTK uses satellite-based positioning (global navigation satellite systems, GNSS) for enhanced precision of measured coordinates. Absolute accuracy from the RTK was 2 cm for horizontal and vertical measurements (Ogaja, 2011, 43).<sup>11</sup> The control points needed to be identifiable so that they could be measured in the imagery. Figure 20 shows how the GCP targets were made from white poster board that was cut into crosses measuring 6 inches from each side and 1.5 ft from cross end to cross end. The targets were laid in the field in an



Figure 20  
Control Point Targets

Note: Measurements made by a Professional Land Surveyor using RTK equipment. Absolute accuracy of measurements was 2 cm.

irregular spacing pattern to provide ground truth in all areas of the project. The crosses were then measured and recorded in UTM Zone 10N horizontal coordinate system. The horizontal datum used was WGS-84. The vertical coordinate system was NAVD 1988. All measurements were recorded in meters. Additionally, 132 checkpoints were surveyed. Figure 21 shows the map of the 9 GCP targets and the 132 checkpoints. The importance of the checkpoints is discussed in Chapter 7.



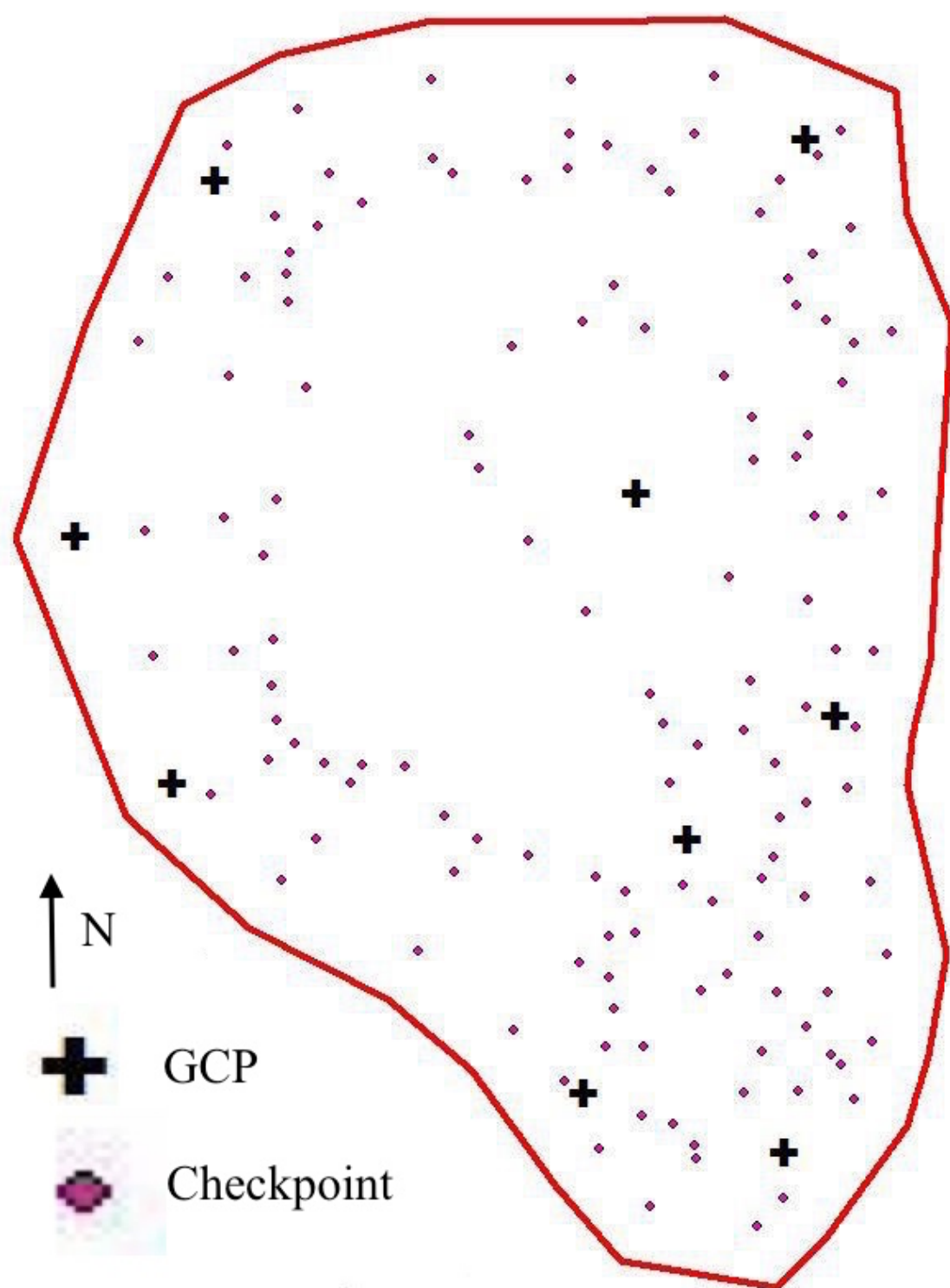


Figure 21  
GCP and Checkpoints Map  
Note: 9 GCPs. 132 Checkpoints

### Part III. Data Processing Methodology

#### Chapter 6 – 3-D Model Construction

Structure from Motion processing technology is well suited for a UAS photogrammetry project. Acquiring 236 images for a 2.5 acre site provided sufficient coverage. The SfM software package used for image processing was Photoscan Pro from Agisoft. Photoscan accepts photographs from any OTS non-metric camera and produces 3-D models and orthophoto mosaics. Ground truthing can be applied using GCPs (Agisoft Photoscan Users Manual, 2013).<sup>17</sup>

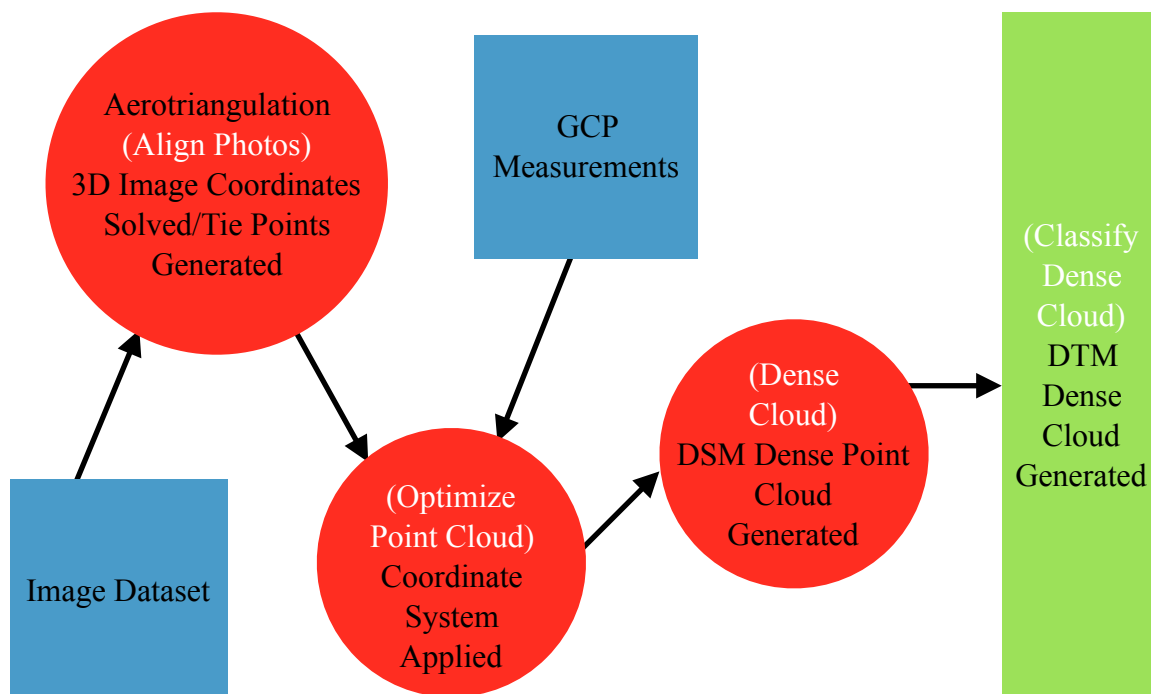


Figure 22

Project Image Processing Workflow Step 1 (All Processing Done in Agisoft Photoscan)

Shape Colors Explained: Blue - Inputs, Red - Outputs, Green - End Solution

Text Color Explained: White - Software Process Name, Black - Product



There are a number of steps involved in the Photoscan workflow that are illustrated in Figure 22. The generated dense point cloud provides a digital surface model (DSM). There are three steps to post processing the dense point cloud, however, for an accurate assessment of the bare-earth. Step one of the post process was to remove all vegetation and above-ground features to create a digital terrain model (DTM) point cloud. This was performed in Photoscan using the “classify dense cloud” tool (green box in Figure 22).

After DTM point cloud generation, step two involved exporting the point cloud in a .las format. Dot las was originally designed for 3-D scanning data or LiDAR and the LAS represents laser (LASer (LAS) File Format Exchange Activities, 2012).<sup>21</sup> Although many characteristics differ between LiDAR and photogrammetry point clouds, software packages that recognize .las will work with both. Step two of the post process was the generation of model key points (MKP). Model key points represent a thinned version of a point cloud maintaining a much smaller amount of points. Key Points are commonly used in LiDAR projects to reduce file size so that data is more manageable. They also provide a better cartographic representation of the ground for contours and other bare-earth products (LAS Specification 1.3, 2010).<sup>22</sup> The MKPs were generated using a tool called “lasthin” from the software vendor LasTools. Figure 23 demonstrates the workflow of the MKP generation.

Step 3 involved extracting the elevation values from the the UAS data. Chapter 7 explains why these values were needed for the model accuracy assessment. Detailed in

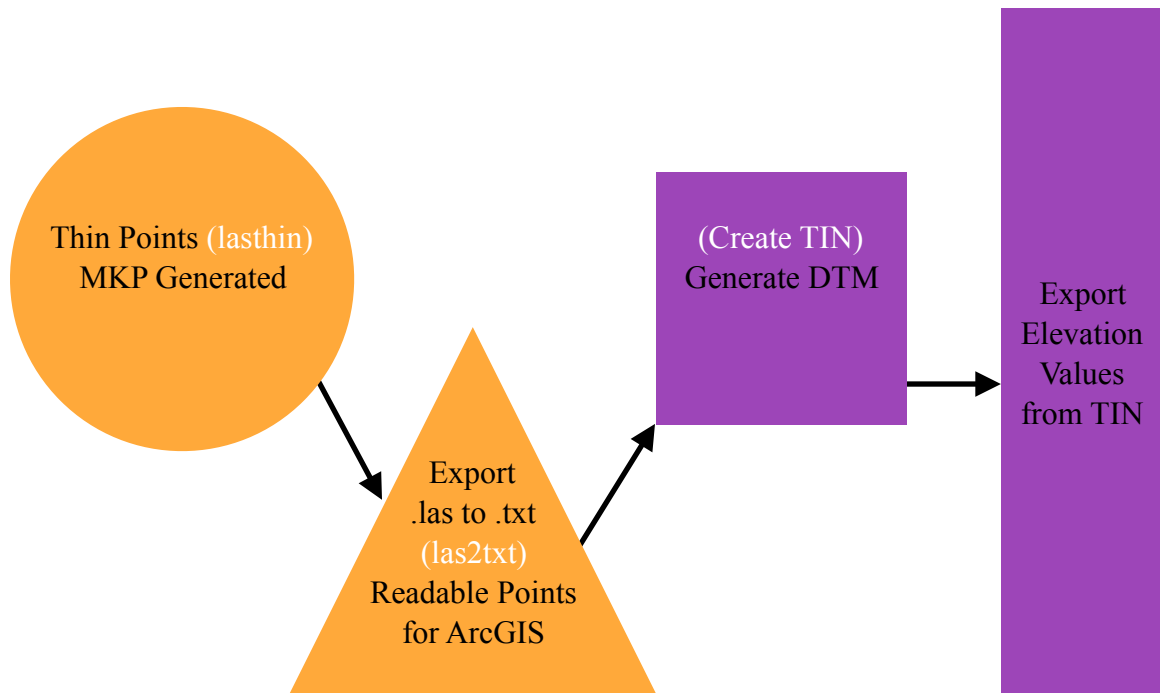


Figure 23

Project Image Processing Workflow Step 2 (MKP Generation) & Step 3 (Elevation Value Extraction)

Shape Colors Explained: Yellow - LASTools MKP Generation, Purple - ArcMap TIN Generation for Extraction of Elevation Values of UAS Data

Text Color Explained: White - Software Process Name, Black - Product

Figure 23, the workflow shows that a TIN of the UAS data was created in ArcMap. The TIN provided elevation data about the UAS derived product. The horizontal location of the elevation values used for accuracy assessment in Chapter 7 were derived from selecting 10 irregularly spaced checkpoints. The checkpoint locations are illustrated on the map in Figure 24.

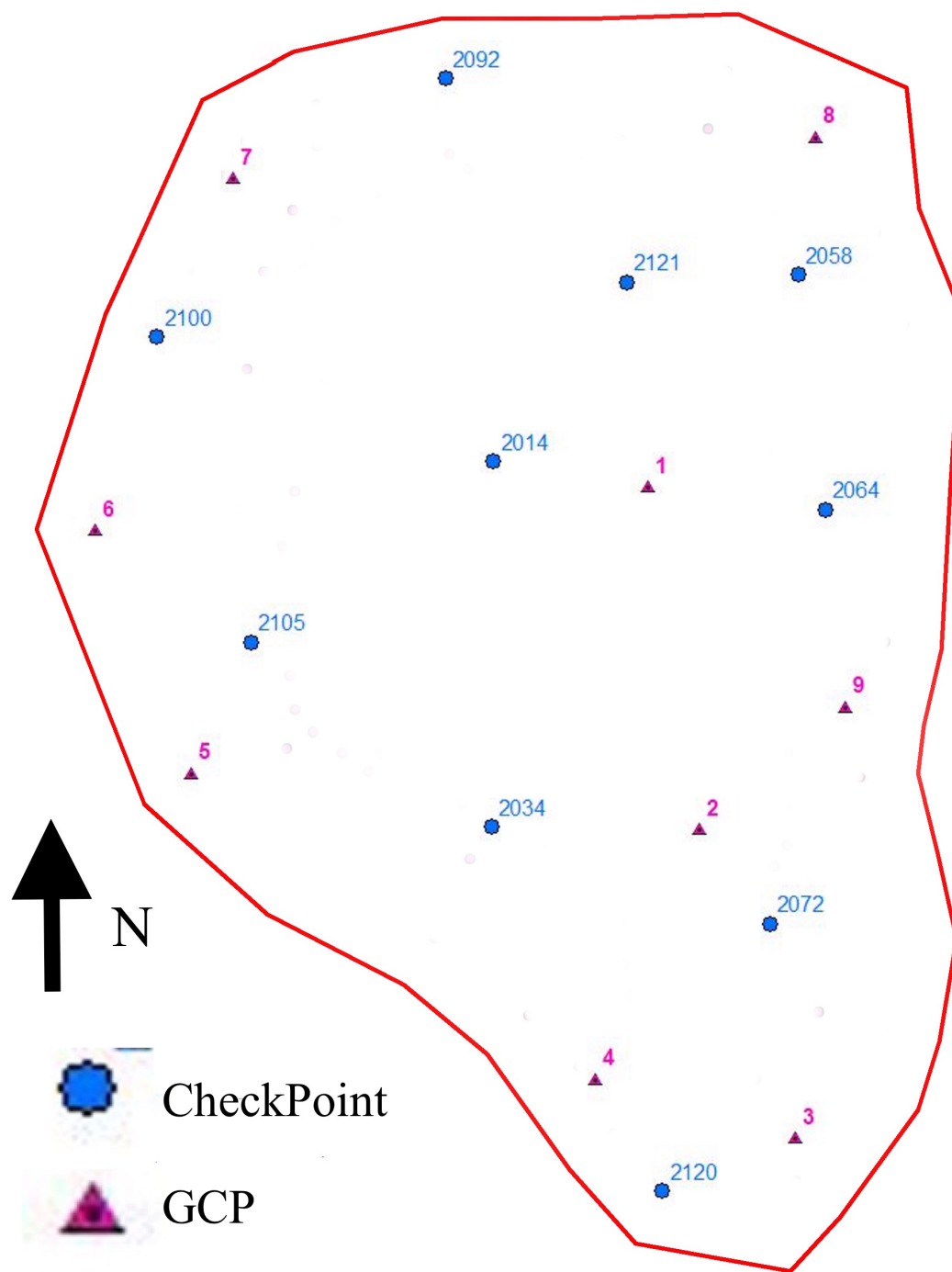


Figure 24

Map of Checkpoints used for Elevation Value Extraction

Note: 10 irregularly spaced checkpoint horizontal locations were used to extract the elevation values from the TIN derived in ArcMap 10.3

## Part IV. Product Assessment

### Chapter 7 – Model Tests/Accuracy Assessment

A number of questions were raised about the integrity of the data after processing it per the recommendations of the software vendor. Was 80% overlap sufficient, not enough, or too much? What would be the effect of reducing the amount of GCPs? Four different DTMs were created in an attempt to evaluate the most efficient and accurate method of UAS photogrammetry. Reducing overlap was done by removing almost half of the images. This reduced the overlap by roughly 30% in most areas. The other test was to remove 4 of control points used for the ground truth. This reduced the number of GCPs from 9 to 5. Table 4 illustrates a breakdown of the characteristics of each model:

Model Number	Number of Images	Number of GCPs	Number of DSM Points	Overlap	Processing Time
Model 01 (M01)	236	9	2.95 Million	70-80%	2.5 Hours
Model 02 (M02)	236	5	2.95 Million	70-80%	2.5 Hours
Model 03 (M03)	129	9	2.6 Million	50-60%	1 Hour
Model 04 (M04)	129	5	2.6 Million	50-60%	1 Hour

Table 4  
Digital Terrain Model Characteristics Breakdown

Three tests were used to assess the accuracy of the 3-D models. First was a coverage test to determine if reducing the overlap would result in gaps in the data.

Models M01 & M02 (M01M02) each generated a DSM point cloud of 2.95 million points. Models M03 & M04 (M03M04) generated 2.6 million points despite having 107 images removed. Except around the perimeter, all models maintained sufficient enough coverage and overlap. In fact, most areas of M0304 were covered by 5-9 images at a time. Figure 25 illustrates the amount of coverage and overlap achieved for M01M02 and M03M04. The black dots in Figure 25 represent the location of each image center. The only way to change image sidelap would be to modify the number of flightlines and fly again. Therefore, all models maintained 40% sidelap. Since M03M04 provide sufficient coverage, it was determined that SfM can be an efficient processing technique with less

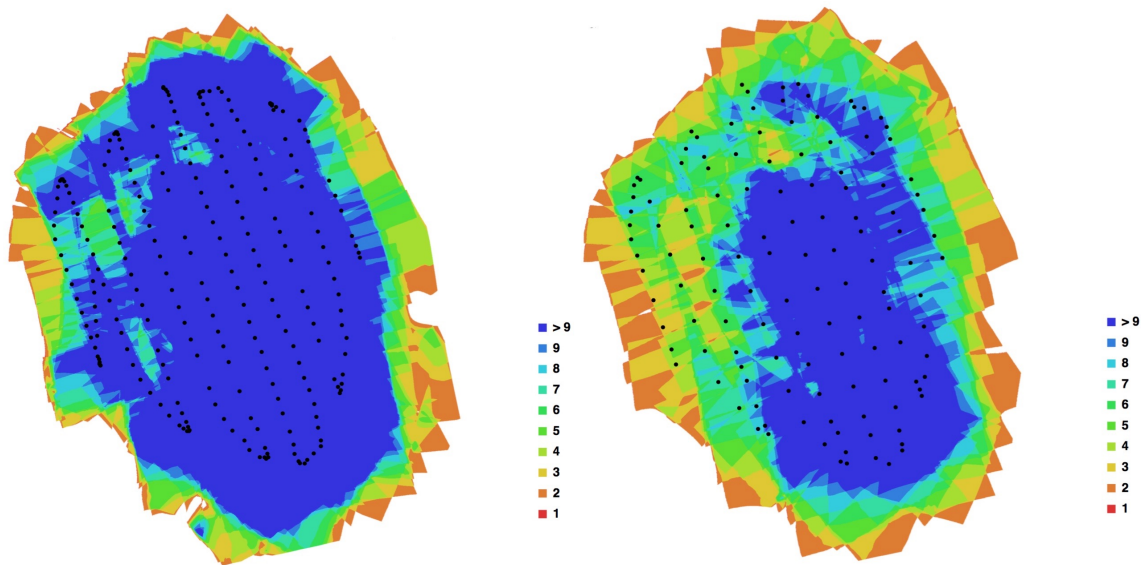


Figure 25

Image Overlap and Coverage

Left: M01M02 - 236 Images

Right: M03M04 - 129 Images

Black Dots Represent Image Center Locations

Colors Explained: Blue - 9+ Photos of Overlap, Green - 5 Photos of Overlap, Orange - 2 Photos of Overlap.

Horizontal Checkpoints	M02	M04
Withheld GCP 2 Residual	0.030	0.018
Withheld GCP 4 Residual	0.097	0.034
Withheld GCP 6 Residual	0.109	0.157
Withheld GCP 8 Residual	0.067	0.110
RMSE	0.082	0.098

Table 5

Horizontal Positional Accuracy

Note: Numbers are in Meters

For an ideal horizontal accuracy assessment, at least 10 or more horizontal checkpoints (n) should be used. This was not an available option for this project.

overlap then the vendor recommends. An important consideration was the time spent processing the data. M0102 took 2.5 hours to process compared to 1 hour for M03M04. Therefore, a reduced amount of overlap was more efficient for this project.

The second test was to determine the offset values of the models with the checkpoints. Horizontal accuracy was determined by finding the root-mean-square error (RMSE) of the horizontal offsets. RMSE is the standard metric used for determining the accuracy of mapping products (ASPRS Positional Accuracy Standards for Digital Geospatial Data, 2014).<sup>23</sup> The lower the RMSE result, the tighter the solution, hence the more accurate it is. The even numbered GCPs were withheld from models M02 and M04 and used as horizontal checkpoints. The GCP targets were then measured in the ortho-mosaic. Those measurements were subtracted from the actual GCP horizontal coordinates to produce residual values. The residuals were then plugged into the following formula:

$$\text{RMSE} = \sqrt{(\sum \text{residuals}) \div n}$$

Table 5 displays the RMSE values of M02 & M04. The table shows that M02, which maintained all 236 images, was 2 cm more accurate in horizontal position than M04, which only used 129 images.

Vertical accuracy was determined by finding the RMSE of the vertical offsets.

The extracted elevation values from the UAS derived TIN in Figure 23 were subtracted

Checkpoint s	Elevation from PLS	Model Elevation Values				Model Residuals			
PointID	Z	M01	M02	M03	M04	M01	M02	M03	M04
2014	71.88	71.92	71.82	71.78	71.91	-0.04	0.06	0.10	-0.03
2034	82.07	82.04	82.00	82.01	82.05	0.03	0.07	0.06	0.02
2058	79.65	79.81	79.89	79.75	79.92	-0.16	-0.24	-0.09	-0.27
2064	75.10	75.21	75.28	75.13	75.40	-0.12	-0.18	-0.04	-0.30
2072	73.09	73.07	73.04	73.07	73.04	0.02	0.05	0.02	0.05
2092	84.98	85.03	85.19	85.13	85.26	-0.05	-0.21	-0.15	-0.28
2100	88.70	88.92	89.09	88.80	88.69	-0.22	-0.40	-0.11	0.01
2105	87.54	87.67	87.63	87.67	87.64	-0.13	-0.09	-0.13	-0.10
2120	72.72	72.60	72.43	72.56	72.40	0.13	0.29	0.17	0.32
2121	74.22	74.16	74.24	73.98	74.16	0.06	-0.03	0.24	0.06
RMSE						0.11	0.20	0.13	0.19

Table 6  
Vertical Positional Accuracy  
Note: Numbers are in Meters

from the 10 checkpoints that were measured by the PLS in Figure 24. The residuals were then plugged into the same formula above to find the RMSEs.

Table 6 demonstrates that models using more control points (M01 vs. M03) had smaller RMSE values, thus tighter accuracy. The difference in horizontal RMSE between M02 and M04 was so small that it cannot be determined if more images makes a significant difference to accuracy. Therefore, Model 03 was determined to be the most accurate and efficient.

Following the latter assessment, model M03 was used for the remaining tests. To extend the assessment of the vertical offsets, the RMSE for all 132 checkpoints were determined for M03. A handful of checkpoints in the northeast area of the project had residual values greater than 0.25. The taller grass caused M03 to float slightly in that vicinity, hence the larger offset. Nevertheless, the vertical RMSE for all 132 checkpoints was 0.16 meters, or 3 cm higher than the 10 checkpoint test.

Finding patterns of the vertical offset was the purpose of test three. The residuals of all 132 checkpoints were plotted on the map shown in Figure 26. Figure 26 illustrates that areas of the DTM that had higher (floating) absolute values than the checkpoints were dispersed throughout the northern portion of the map. Areas of lower (digging) absolute values were found in the far southern region of the map. The map suggests that the model was floating at the crest of the quarry where absolute elevations were higher than the base. Dense vegetation was more prevalent along the crest, another suggested



cause of the floating offsets (ASPRS Positional Accuracy Standards for Digital Geospatial Data, 2014).<sup>23</sup>

Figure 27, however, gives a more qualitative evaluation of the vertical offset values. Floating residuals were dispersed at all absolute elevations suggesting no correlation exists. But digging residuals only occurred in lower absolute elevations. Since

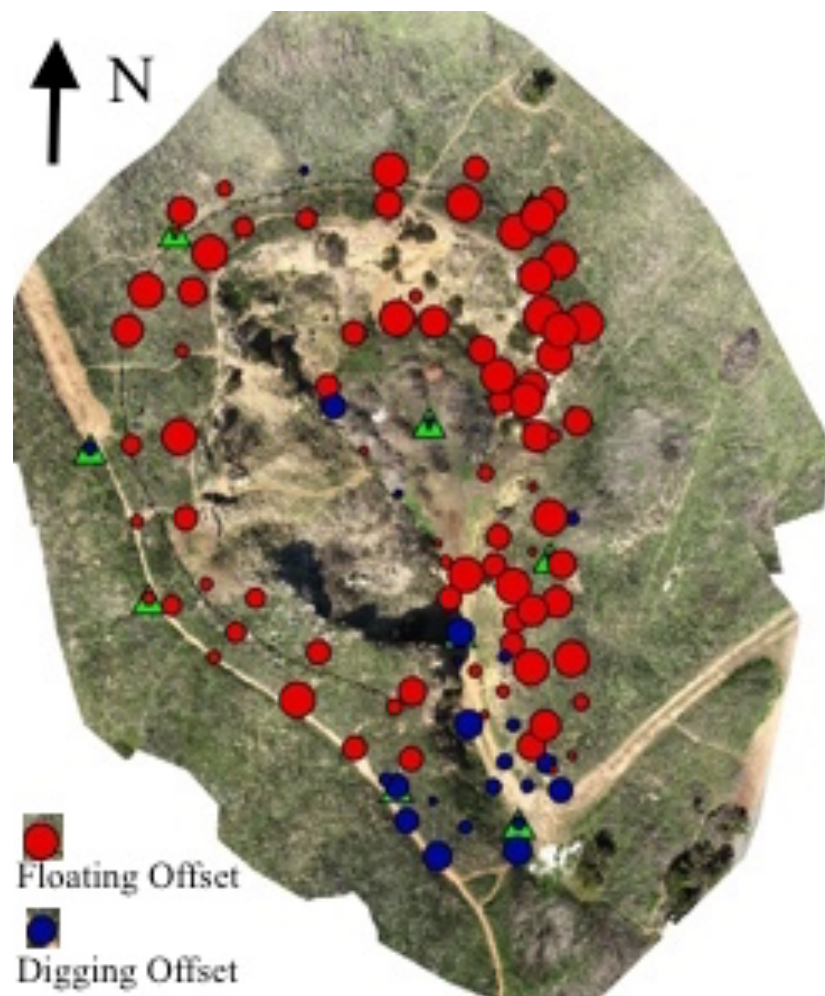


Figure 26

Vertical Offsets Mapped

Colors Explained:

Red - UAS DTM values were higher than checkpoints or “floating”

Blue - UAS DTM values were lower than checkpoints of “digging”

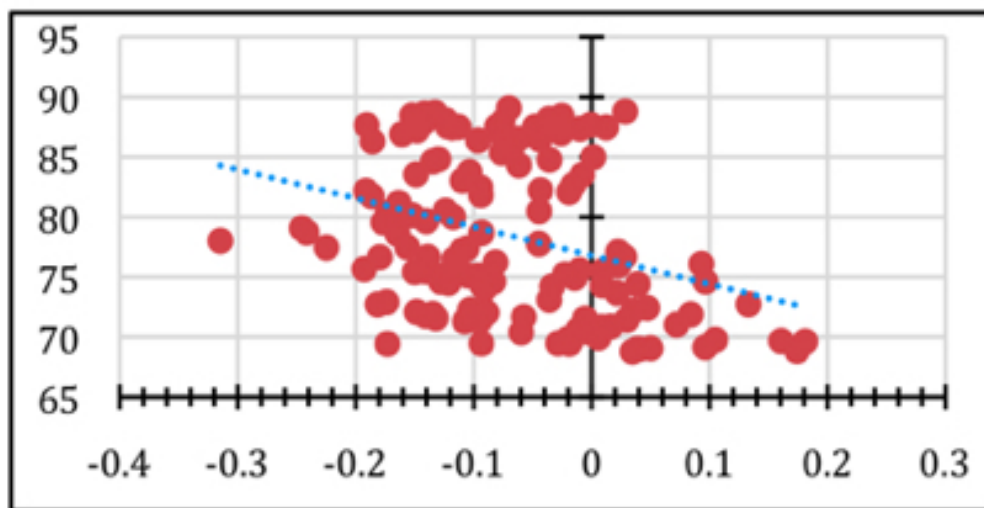


Figure 27

#### Vertical Residuals vs. Absolute Heights

Explanation: Red dots represent UAS TIN elevation values. The X axis represents the residual elevation values in meters. The Y-axis represents absolute values. The graph illustrates that no trend for residuals that were floating. But residuals that were digging trend towards being located near the base of the model.

the lowest elevations were at the base and southern area, it can be determined that a stretch of the model occurs. That is, the SfM software overcompensated when major changes in absolute elevation occurred.

Figure 28 shows that a TIN model of the checkpoints was then created to visualize the fit between the checkpoints and M03. The TINs were converted to rasters and the Minus tool was used in ArcGIS. The raster comparison determined that the models fit within a meter except in areas of steep slopes where no checkpoints were recorded. This is demonstrated in Figure 29. The stretch phenomena is also present as the base of the quarry is consistently digging and the crest floating.

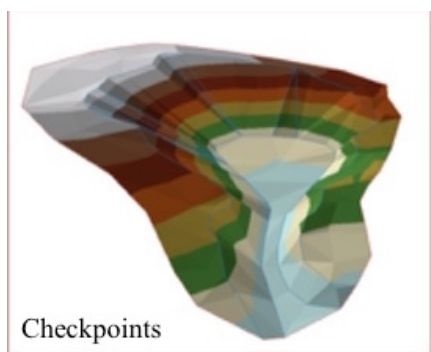
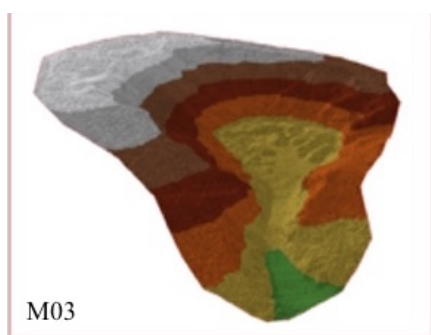


Figure 28  
M03 TIN (Top) vs.  
Checkpoints TIN (Bottom)  
Explanation: TINs created for  
subtraction method. M03  
displays more terrain  
information was collected from  
the UAS than the traditional  
survey.

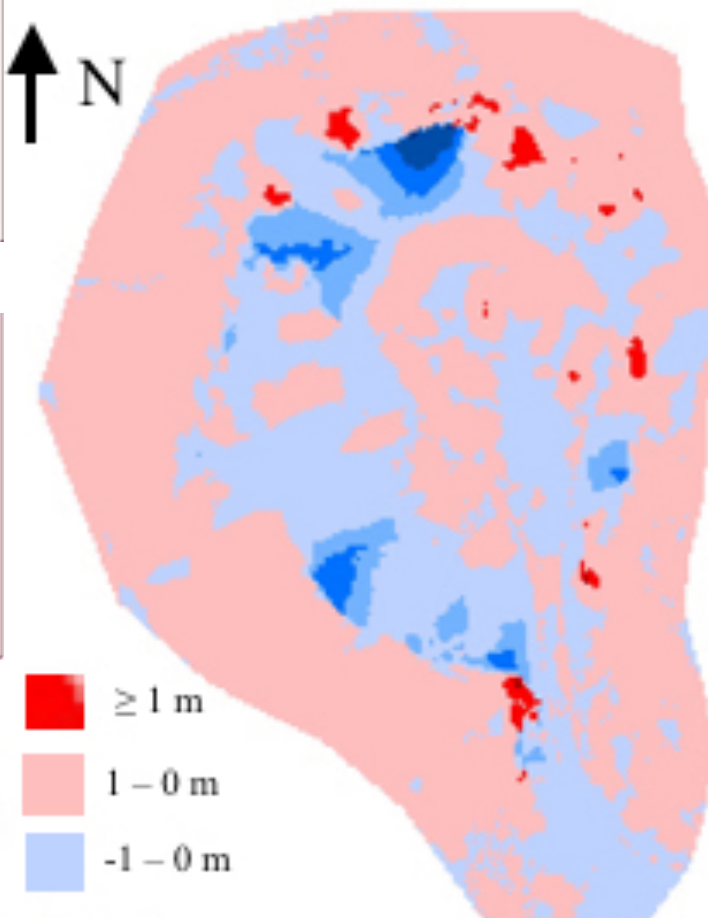


Figure 29  
M03 vs. Checkpoints Change Map  
Explanation: Minus tool in ArcMap was used  
to visualize the subtraction of M03 and the  
checkpoints. Darker colors represent larger  
vertical offsets.

## Chapter 8 – Image Quality

Since its introduction, Apple consistently upgrades the quality of the iPhone's camera. During the spring of 2014, the iPhone 5S model camera ranked at the top of numerous consumer reports. Time and again, Apple has proven that it can produce a cell phone camera capable of taking superb pictures for the casual user.

Mounting an iPhone to a UAS proved challenging. Initial mounting tests included using duct tape, a workout armband, musical instrument vibration reduction material, and rubber bands. Each iteration provided the same results. Photos came out smeared and blurry about 90% of the time. The camera's CMOS rolling shutter sensor combined with the vibrations of the quadcopter motors were causing a jello effect (Garrison,

2015).<sup>24</sup> Jello refers to linear features appearing wobbly or not straight as if the image was resting on a bowl of jello. An example of jello can be found in Figure 30.

Drone manufacturers were aware of this phenomena and developed special anti-vibration mounts to remedy. The mount includes two plates separated by rubber

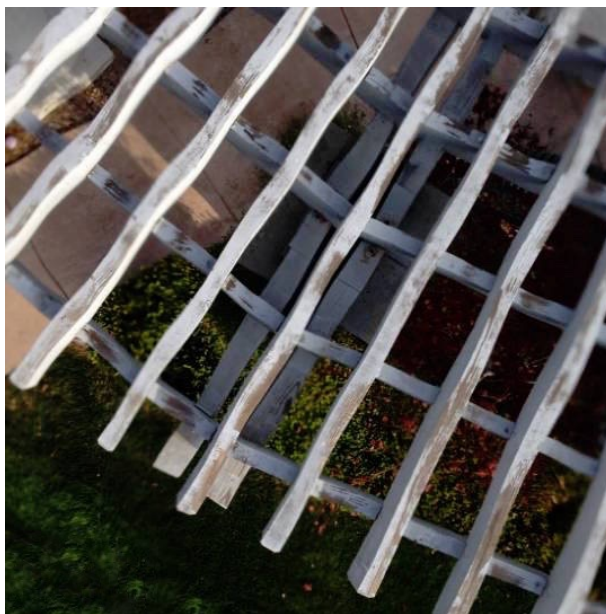


Figure 30  
Jello Effect on Image Quality  
Explanation: Areas of the image that are blurred or warped caused by vibrations, a slow rolling shutter, or both. Jello was present throughout the ortho mosaic of this project.

dampeners. According to Garrison, the dampeners were supposed to reduce the jello significantly (Garrison, 2015).<sup>24</sup> The iPhone mount was bolted to an anti-vibration mount produced by DJI. Figure 16 in Chapter 4 illustrates the iPhone mount for this project. After flying the UAS with the new mount, the majority of the larger jello artifacts were removed. It was not until further inspection (while zoomed in for GCP measurement) that much smaller traces of jello were present. Chapter 7 demonstrated that the iPhone camera was capable of producing accurate 3-D models. Assessment of the orthophoto mosaic, however, proved otherwise. Months of flight testing did not fix the small scale jello, and it was determined that the low quality rolling shutter and slow processing camera sensor of the iPhone 5S would always cause this problem.



## Chapter 9 – Mapping Solutions

Unmanned systems photogrammetry allows for the production of a number of flexible mapping solutions (Colomina et al., 2014, 81).<sup>12</sup> Shown below, Figures 31-34 were produced from this project and provide a brief list of applications:



Figure 31

Derived Mapping Solution - Orthophoto Mosaic

Applications: Basemaps, Engineering Design Work, Planning, Site Monitoring, Image Classification, Change Detection





Figure 32

Derived Mapping Solution - Point Clouds

Applications: DSM Generation, DTM Generation, Vegetation Monitoring, Volume Calculations



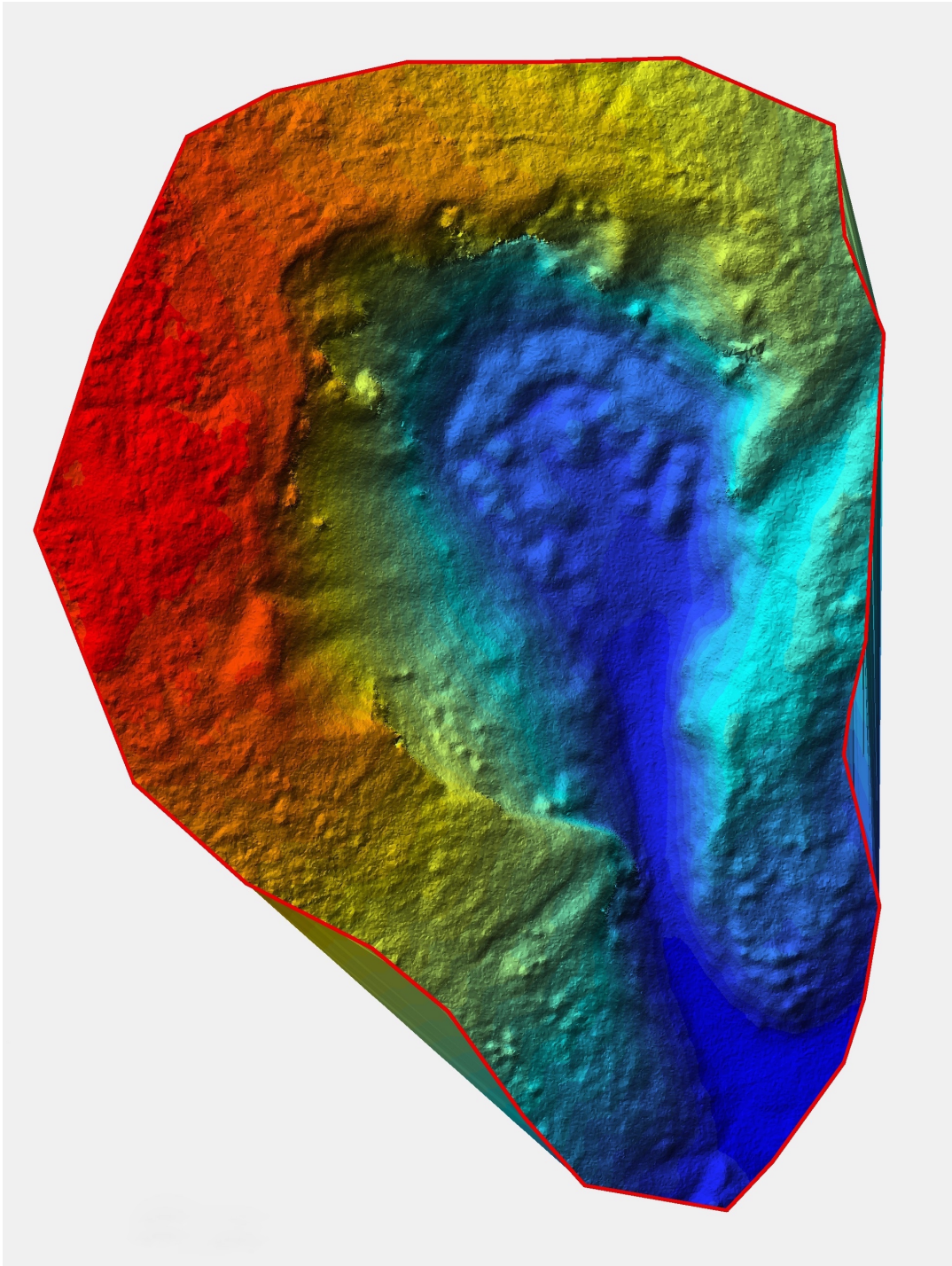


Figure 33  
Derived Mapping Solution - Digital Terrain Model  
Applications: Contour Generation, Slope Analysis, Disaster Monitoring, Engineering Blueprints



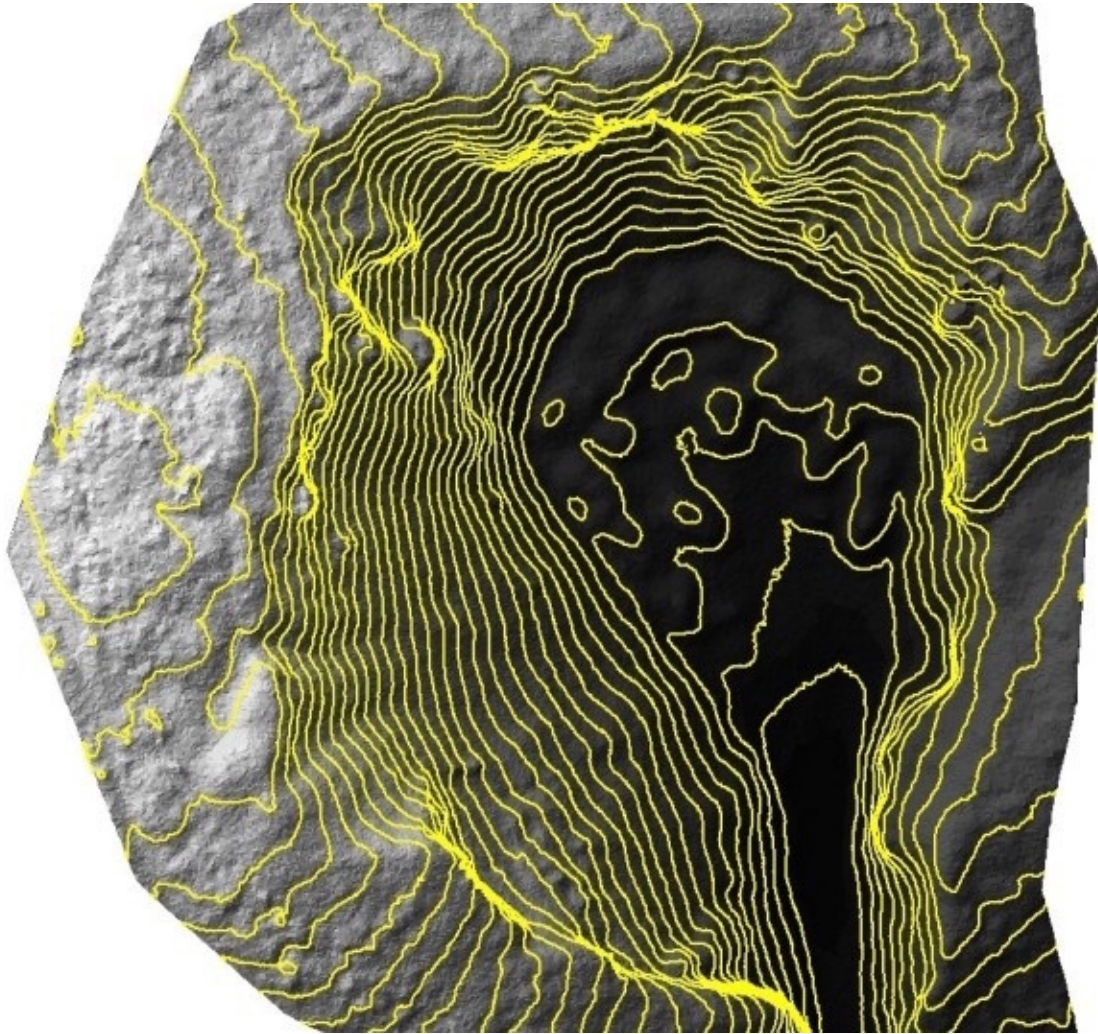


Figure 34

Derived Mapping Solution - Contours

Applications: Topographic Modeling, Engineering Design, Height Measurements, Hydrographic Surveys, Land Surveyor Support

## **Part V. Future Recommendations**

Although UAS provide the opportunity for finer resolution data, it doesn't necessarily mean the data is better. Unless needed for very small feature detection, this author found that a 1 cm GSD was overkill. The quarry sight was only 2.5 acres in size, yet needed over 100 images to have sufficient coverage. Increasing the GSD just 1 cm more would ensure a significantly less amount of photos would be needed and the coverage area would also increase.

An ortho mosaic should have its color balanced and consistent. Since cameras are passive sensors, they are completely reliant on the amount of light that is reflected back to them. It takes time in the field to acquire hundreds of images, and the slightest change in sun angle, cloud cover, or other weather related factor can have an impact on the exposure consistency (Lillesand, et al., 2008, 123).<sup>4</sup> This rule is even more true in winter months. UAS are very dependent on consistent weather and sun conditions to produce a reliable product.

While capable of producing highly accurate topographic mapping solutions, the iPhone 5S camera fell short of producing high-quality (artifact free) photographs on a consistent bases. Since this research began in 2013, numerous drone vendors have developed RTF systems with built on cameras (DJI Phantom 3 Professional, 2016).<sup>25</sup> Initially designed for recreation, these systems are being used for mapping research and are proving to be capable of producing high-quality/accuracy solutions (Gómez et al.,

2013).<sup>26</sup> Although quadcopters continue to dominate the drone market, fixed-wing and hybrid platforms are also proving valuable for large area mapping applications.

Flying the site again under different flight parameters could generate different results. How would the data act with more/less sidelap? How would it perform if the flightlines were planned in an East/West configuration instead of North/South? What about a combination of both? Different flight characteristics could have a significant influence on the accuracy outcome.

The photogrammetry application spawned a number of start-up software companies in the U.S. and internationally. Agisoft is based in Russia. Pix4D, it's largest competitor, is based in Switzerland. Mapping stalwarts like Trimble, QCoherent, and TopCon have also jumped on the SfM bandwagon. The drone market is not limited to just hardware manufacturers as many of these companies are seeking turn-key mapping packages that include the UAS, software, and cloud support. Subscription services like Drone Deploy and MapsMadeEasy exist as well for users that have their own system but don't have the knowledge, time, or resources to purchase photogrammetry software. This is a new phenomena and something never offered before in the CP world.

Are any of these packages or services better than the methodology presented in this paper? This author believes that there is not a definite yes or no answer. Turn-key packages from reliable vendors will produce data that is comparable or better. But those systems can cost upwards of \$50,000. The high price of these systems is due to manufacturers upselling platforms made from industrial grade components or other buzz-

worthy terms. And this research has determined that the sensor has a much larger impact on the quality of the mapping product, while the platform plays a much smaller role.

Subscription based photogrammetry is done through the cloud making it a black-box solution with little to no quality control checks. How is that data vetted? It is the opinion of this author that companies providing these services are making maps that are good “enough” instead of products that meet traditional standards. Drones, however, have unlocked new markets like precision ag, real estate, etc., where survey grade solutions are not required by the user. The next logical research would be to conduct a comprehensive test of many of these systems and services.

## **Part VI. Conclusion**

From the film cameras to drones, photogrammetry has evolved into a major discipline of remote sensing. Aerial mapping was established as an invaluable military asset in WWI. Civilian photogrammetry gained momentum following the war, and by the turn of the millennium, photogrammetry became an analytically automated and digital resource for conducting survey and mapping. The industry has undergone a paradigm shift in recent years thanks to the introduction of drones and SfM processing software. While conventional photogrammetry remains relevant, UAS photogrammetry is disrupting the status quo.

This research explored the idea of UAS photogrammetry from a consumer grade drone and an iPhone 5S camera. Numerous conventional principles were applied, and new processing methods like SfM were explored. Image quality was poor and not recommended for producing an orthophoto mosaic. But the system was capable of producing high-accurate 3-D models useful in numerous applications. It was concluded that the sensor has a much larger impact on the quality of data than the drone itself. A future recommendation would be to test different sensors, turn-key systems, and processing service providers.

## References

1. "Man Shoots Down Drone Hovering over House." 2015. *CNET*. Accessed 09 August 2015. <http://www.cnet.com/news/man-shoots-down-drone-hovering-over-house/>
2. Anderson, C. "Drones: When the Future Sneaks Up on You." 2013. *Linked-In*. Accessed 02 January 2016. <http://www.linkedin.com/today/post/article/20130429052618-9966-drones-when-the-future-sneaks-up-on-you?trk=prof-post>
3. "A Look Back." 2007. *Photogrammetric Engineering and Remote Sensing*. Accessed 28 December 2015. <http://www.asprs.org/a/publications/pers/2007journal/may/lookback.pdf>
4. Lillesand, T., Keifer, R., & Chipman, J. 2008. *Remote Sensing and Image Interpretation 6th Edition*. New Delhi, India. John Wiley & Sons, Inc.
5. "History of Aerial Photography." 2015. *Professional Aerial Photographers Association*. Accessed 22 August 2015. [http://professionalaerialphotographers.com/content.aspx?page\\_id=22&club\\_id=808138&module\\_id=158950](http://professionalaerialphotographers.com/content.aspx?page_id=22&club_id=808138&module_id=158950)
6. McGlone, C., Mikhail, E., Bethel, J., & Mullen, R. 2004. *Manual of Photogrammetry Fifth Edition*. Bethesda, MD.: American Society of Photogrammetry and Remote Sensing.
7. "ASPRS Mission Statement." 2015. *American Society of Photogrammetry and Remote Sensing*. Accessed 29 December 2015. <http://www.asprs.org/About-Us/Mission-Statement.html>
8. Guarneri, J. "History of Photogrammetry." 2012. *Prezi*. Accessed 28 December 2015. <https://prezi.com/-9fivl3b0zle/history-of-photogrammetry/>
9. Falkner, E., Mrogan, D. 2002. *Aerial Mapping: Methods and Applications*. Boca Raton, FL. CRC Press LLC.
10. "Minimum Safe Altitudes." 2002. *Flight Training*. Accessed 29 December 2015. [http://flighttraining.aopa.org/magazine/2002/January/200201\\_Training\\_Topics\\_Legal\\_Briefing.html](http://flighttraining.aopa.org/magazine/2002/January/200201_Training_Topics_Legal_Briefing.html)
11. Ogaja, C. 2011. *Geomatics Engineering: A Practical Guide to Project Design*. Boca Raton, FL. CRC Press LLC.

12. Colomina, I., Molina, P., 2014. "Unmanned Aerial Systems for Photogrammetry and Remote Sensing: A Review." *ISPRS Journal of Photogrammetry and Remote Sensing*. 92, 79-97.
13. "Leica RC30 Aerial Camera System." 2016. *Leica-Geosystems*. Accessed 02 January 2016. [http://w3.leica-geosystems.com/downloads123/zz/airborne/rc30/documentations/RC30\\_product\\_description.pdf](http://w3.leica-geosystems.com/downloads123/zz/airborne/rc30/documentations/RC30_product_description.pdf)
14. Crisp, S. "Camera Sensor Size: Why Does it Matter and Exactly How Big Are They?" 2013. *Gizmag*. Accessed 02 January 2016. <http://www.gizmag.com/camera-sensor-sizeguide/26684/>
15. Westoby, M.J., Brasington, J., Glasser, N.F., Hambrey, M.J., Reynolds, J.M. "Structure-from-Motion Photogrammetry: A Low-Cost, Efficient Tool for Geoscience Applications." 2012. *Geomorphology*. Accessed 30 December 2015. <http://www.sciencedirect.com/science/article/pii/S0169555X12004217>
16. Snavely, N., Seitz, S.N., Szeliski, R., 2008. "Modeling the world from internet photo collections." *International Journal of Computer Vision*. 80, 189–210.
17. "Agisoft Photoscan Users Manual Version 1.0." 2013. *Agisoft*. Accessed 02 January 2016. [http://downloads.agisoft.ru/pdf/photoscan-pro\\_1\\_0\\_0\\_en.pdf](http://downloads.agisoft.ru/pdf/photoscan-pro_1_0_0_en.pdf)
18. "IRIS+." 2016. *3DR Store*. Accessed 02 January 2016. <https://store.3drobotics.com/products/iris>
19. "Lime Ridge Open Space." 2012. City of Walnut Creek Accessed 31 December 2015. <https://www.youtube.com/watch?v=bCzT86BZdfU>
20. "CameraSharp." 2015. *Screensmudge, LLC*. Accessed 04 January 2016. <http://www.screensmudge.com/camerassharp/>
21. "LASer (LAS) File Format Exchange Activities." 2012. *American Society of Photogrammetry and Remote Sensing*. Accessed 04 January 2016. <http://www.asprs.org/Committee-General/LASer-LAS-File-Format-Exchange-Activities.html>

22. "LAS Specification Version 1.3." 2010. *American Society of Photogrammetry and Remote Sensing*. Accessed 04 January 2016. [http://www.asprs.org/a/society/committees/standards/LAS\\_1\\_3\\_r11.pdf](http://www.asprs.org/a/society/committees/standards/LAS_1_3_r11.pdf)
  
23. "ASPRS Positional Accuracy Standards for Digital Geospatial Data." 2014. *American Society of Photogrammetry and Remote Sensing*. Accessed 04 January 2016. [http://www.asprs.org/a/society/committees/standardsASPRS\\_Positional\\_Accuracy\\_Standards\\_Edition1\\_Version100\\_November2014.pdf](http://www.asprs.org/a/society/committees/standardsASPRS_Positional_Accuracy_Standards_Edition1_Version100_November2014.pdf)
  
24. Garrison, K., "Reducing Jello and Getting a More Natural Look in Your Aerial Video." 2015. *Drone Tech Report*. Accessed 04 January 2016. <http://dronetechreport.com/reducing-jello-getting-natural-look-aerial-video/>
  
25. "DJI Phantom 3 Professional." 2016. *DJI*. Accessed 04 January 2016. <http://www.dji.com/product/phantom-3-pro>
  
26. Gómez-Candón, D., De Castro, A.I., & López-Granados, F. "Assessing the Accuracy of Mosaics from Unmanned Aerial Vehicle (UAV) Imagery for Precision Agriculture Purposes in Wheat." 2013. *Precision Agriculture*. Accessed 04 January 2016. <http://link.springer.com/article/10.1007/s11119-013-9335-4#/page-1>